

# Gamma-ray Burst 080319B: Evidence for Relativistic Turbulence, Not Internal Shocks

Pawan Kumar<sup>1</sup> & Ramesh Narayan<sup>2</sup>

<sup>1</sup>Astronomy Department, University of Texas, Austin, TX 78712

<sup>2</sup>Harvard-Smithsonian Center for Astrophysics, 60 Garden Street, Cambridge, MA 02138

## ABSTRACT

We show that the excellent optical and gamma-ray data available for GRB 080319B rule out the internal shock model for the prompt emission. The data instead point to a model in which the observed radiation was produced close to the deceleration radius ( $\sim 10^{17}$  cm) by a turbulent source with random Lorentz factors  $\sim 10$  in the comoving frame. The optical radiation was produced by synchrotron emission from relativistic electrons, and the gamma-rays by inverse Compton scattering of the synchrotron photons. The gamma-ray emission originated both in eddies and in an inter-eddy medium, whereas the optical radiation was mostly from the latter. Therefore, the gamma-ray emission was highly variable whereas the optical was much less variable. The model explains all the observed features in the prompt optical and gamma-ray data of GRB 080319B. We are unable to determine with confidence whether the energy of the explosion was carried outward primarily by particles (kinetic energy) or magnetic fields. Consequently, we cannot tell whether the turbulent medium was located in the reverse shock (we can rule out the forward shock) or in a Poynting-dominated jet.

*Subject headings:* radiation mechanisms: non-thermal — relativistic turbulence  
— gamma-rays: bursts

## 1. Introduction

Two major unsolved questions in the field of gamma-ray bursts are: (i) the mechanism by which the energy in relativistic jets is converted to random particle kinetic energy, and (ii) the radiation process by which the particle energy is converted to gamma-ray photons.

A number of ideas have been proposed for the conversion of jet energy to particle energy (cf. Piran 1999, 2005; Mészáros 2002; Thompson 1994, 2006; Lyutikov & Blandford

2003; Zhang 2007). Most popular among these is the so-called internal shock model (Piran, Shemi & Narayan 1993; Rees & Meszaros 1994; Katz 1994), in which different parts of the relativistic GRB jet travel at different speeds. Faster segments collide with slower segments in shocks, and a fraction of the jet kinetic energy is converted to thermal energy. Gamma-rays are then produced by either the synchrotron process or the synchrotron-self-Compton (SSC) process (e.g., Piran 2005, Mészáros 2002, Zhang 2007). Another model is the external shock model (Dermer 1999) in which gamma-rays are produced via the synchrotron process in an external shock driven into the circumstellar medium by the GRB jet. Difficulties with this model have been pointed out by a number of authors (cf. Piran 1999).

The excellent data obtained by the Swift and Konus satellites for GRB 080319B – dubbed the “the naked eye burst” – has provided a new opportunity to investigate the viability of these models and to understand the fundamental nature of GRBs. We summarize here the main observational properties of this burst (details may be found in Racusin et al. 2008).

GRB 080319B lasted for about 50 s and had a burst fluence in the 20 keV – 7 MeV band of  $5.7 \pm 0.1 \times 10^{-4}$  erg cm<sup>-2</sup>, which corresponds to an isotropic energy release of  $E_\gamma = 1.3 \times 10^{54}$  erg (Golenetskii et al. 2008) for a redshift  $z = 0.937$  (Vreeswijk et al 2008; Cucchiara & Fox 2008). The time-averaged gamma-ray spectrum during the burst had a peak at around 650 keV. The maximum flux at this energy was  $\sim 7$  mJy, and the time averaged flux was  $\sim 3$  mJy. The time-averaged gamma-ray spectrum was measured by Konus-Wind (Racusin et al. 2008) to be  $F_\nu \propto \nu^{0.18 \pm 0.01}$  for photon energies below 650 keV and  $F_\nu \propto \nu^{-2.87 \pm 0.44}$  at higher energies. (The spectrum evolved during the course of the burst, as we discuss in §2, and this provides additional information on the radiation process.) In the optical band, at photon energies around 2 eV, the peak flux of GRB 080319B was  $V = 5.4$  mag or 20 Jy, and the time-averaged flux was about 10 Jy (Karpov et al 2008). The optical lightcurve varied on a time scale of about 5 s, while the  $\gamma$ -ray flux varied on time scales of  $\sim 0.5$  s.

GRB 080319B has seriously challenged our understanding of gamma-ray bursts. The problems posed by this burst are described in Kumar & Panaitescu (2008) and discussed in further detail in the present paper. We show that the observations cannot be explained with any of the standard versions of the internal shock model. We find, however, that a consistent model is possible if we give up the idea of internal shocks and instead postulate that the gamma-ray source is relativistically turbulent (see Narayan & Kumar 2008).

We begin in §2 by arguing that the radiation in GRB 080319B must have been produced by the SSC mechanism. Following this, we derive in §3 the basic equations describing a GRB that radiates via SSC. In §4, we combine these equations with the internal shock model and

attempt to explain the data on GRB 080319B. We find that no consistent model is possible. In §5, we consider a relativistically turbulent model, again with SSC radiation, and show that in this case it is possible to obtain a consistent model of GRB 080319B. We summarize the main conclusions in §6. The Appendix discusses the effects of source inhomogeneity on our calculation of the synchrotron self-absorption frequency, and the synchrotron and inverse-Compton fluxes.

## 2. Why synchrotron-self-Compton model?

Racusin et al. (2008; Fig. 3) and Woźniak et al. (2008; Fig. 4) show that the  $\gamma$ -ray and optical lightcurves (LCs) of GRB 080319B have a similar general shape (although the  $\gamma$ -ray LC is a lot more variable than the optical LC). This suggests that the optical and  $\gamma$ -ray radiation were produced by the same source. An independent theoretical argument in support of this conclusion is given in §4.1. The radiation mechanisms in the two bands must, however, be different since the optical flux is larger by a factor  $\sim 10^4$  than the  $\gamma$ -ray flux extrapolated to the optical band.

The average spectral properties of GRB 080319B were summarized in §1. Racusin et al. (2008; supplementary material – Table 1) also reported spectral fits corresponding to three independent time segments of the burst:  $-2$  s to 8 s, 12 s to 22 s, 26 s to 36 s (all times measured with respect to the nominal start time of the burst). The peak of the gamma-ray spectrum evolved from about 750 keV early in the burst to about 550 keV at late times, giving a mean peak energy of 650 keV as mentioned earlier. More interestingly, the spectral slope at energies below the peak evolved with time:  $F_\nu \propto \nu^{0.50 \pm 0.04}, \nu^{0.17 \pm 0.02}, \nu^{0.10 \pm 0.03}$ , during the three time segments. The unusually hard spectrum during the first time segment unambiguously points to an SSC origin for the gamma-ray emission, as we now argue.

The hardest spectrum possible with optically thin synchrotron emission is  $F_\nu \propto \nu^{1/3}$ . The only way to obtain a harder spectrum is to invoke self-absorption, in which case the spectrum will switch to  $F_\nu \propto \nu^2$  below the self-absorption break. However, in order to obtain a synchrotron spectrum with a mean spectral index of 0.5 in the band between 20 keV and 650 keV, we would need to have the self-absorption break at an energy  $\sim 50 - 100$  keV. This has two serious problems. First, it is virtually impossible to push the self-absorption break to such a large energy with any reasonable parameters for the radiating medium<sup>1</sup>. Second, a

---

<sup>1</sup>For the synchrotron self-absorption frequency to be  $\sim 50$  keV and the flux at 650 keV to be  $\sim 10$  mJy, the distance of the source from the center of the explosion must be less than  $10^8$  cm. At such a small radius the medium would be extremely opaque to Thomson scattering and  $\gamma + \gamma \rightarrow e^+ + e^-$ . Therefore, the

spectral break in which the slope changes from 1/3 to 2 would almost certainly be detectable in the data and would not be consistent with a single power-law with a slope of 0.5.

A Comptonization model gets around these difficulties. If the gamma-ray emission is produced by Compton-scattering, then any break in the spectrum is not intrinsic to the gamma-rays but merely a reflection of a break in the spectrum of the underlying soft photons. If the soft photons are in the optical-infrared band and are produced by synchrotron emission, then the self-absorption break must be around 0.1 eV, which is perfectly compatible with reasonable model parameters. In addition, although the synchrotron spectrum below the break would be very hard, viz.,  $F_\nu \propto \nu^2$ , the corresponding segment in the up-scattered inverse-Compton radiation would be softer:  $F_\nu \propto \nu$  (Rybicki & Lightman, 1979). Thus, the gamma-ray spectrum would break from a slope of 1/3 to 1, which is consistent with the observations, especially when we allow for a smooth rollover from one spectral slope to the other over a range of energies.

Why did the gamma-ray spectral slope below 650 keV switch to  $\sim 0.1-0.2$  at later times? The likely explanation is that the self-absorption frequency of the synchrotron emission dropped to yet lower energies (in the infrared), and so the break in the gamma-ray band was pushed closer to, or even below, 20 keV.

In this discussion, we have assumed that the soft radiation is produced by the synchrotron process. The alternative is thermal radiation, but this can be ruled out as it requires a Lorentz factor of  $\sim 10^8(\delta t)^{-1}T_5^{-1/2}$  to explain the observed flux of 10 Jy <sup>2</sup>; here  $\delta t$  is the observed variability time (in seconds) of the optical lightcurve and  $T_5 = T/10^5\text{K}$  is the temperature of the source. The parameter  $T_5$  cannot be much larger than unity since the total energy release would become excessive ( $> 10^{55}$  erg). A Lorentz factor of  $10^8$  is not reasonable either. Therefore, a thermal model for the optical emission is ruled out.

We thus conclude that the optical photons in GRB 0803019B were produced by the synchrotron mechanism, and the gamma-ray photons were produced by the same relativistic electrons by inverse-Compton scattering the synchrotron photons. That is, all the observed radiation in GRB 0803019B was the result of the SSC process (§4 gives a more detailed discussion).

---

emergent radiation would be thermal and no photons with energy  $\gtrsim 1$  MeV would be able to escape from the source. However, Konus-Wind detected  $\sim 10$  MeV photons from GRB 0803019B.

<sup>2</sup>For a relativistically moving thermal source with a temperature  $T$  (in the observer frame) and radius  $R$ , the observed flux in the optical band at a frequency  $\nu_{op} \sim 5 \times 10^{14}$  Hz is:  $f_{op} \approx 2kT(1+z)^4\nu_{op}^2R^2/(d_L^2c^2\Gamma^2) \approx 2kT(1+z)^2\nu_{op}^2(\delta t)^2\Gamma^2/d_L^2$ . Therefore, to explain the observed optical flux of 10 Jy we require  $\Gamma \sim 10^8(\delta t)^{-1}T_5^{-1/2}$ .

### 3. Synchrotron and SSC processes for a relativistic transient source: basic equations

We first determine what properties the source of optical emission in GRB 080319B must have, assuming that the radiation is produced by synchrotron emission (§3.1). We then consider the gamma-ray data and describe the additional constraints they provide (§3.2). Detailed application to GRB 080319B is discussed in §4 and §5.

#### 3.1. Modeling the prompt optical data

The properties of a synchrotron source can be described by five parameters:  $B$ ,  $N_e$ ,  $\Gamma$ ,  $\gamma_i$  and  $\tau_e$ , which are the magnetic field strength, the total number of electrons, the bulk Lorentz factor of the source with respect to the GRB host galaxy, the *typical* electron Lorentz factor in the comoving frame of the source (the electron distribution is  $dn_e/d\gamma \propto \gamma^{-p}$  for  $\gamma > \gamma_i$ ), and the optical depth of the source to Thomson scattering<sup>3</sup>. If the source is at redshift  $z$ , the peak frequency  $\nu_i$  of the synchrotron spectrum and the observed flux  $f_i$  at the peak, both as seen by the observer, are given by (Rybicki & Lightman, 1979)

$$\nu_i = \frac{\phi_\nu(p)qB\gamma_i^2\Gamma}{2\pi m_e c(1+z)} = (1.15 \times 10^{-8} \text{ eV}) \phi_\nu B \gamma_i^2 \Gamma (1+z)^{-1}, \quad (1)$$

$$f_i = \frac{\sqrt{3}\phi_f(p)q^3BN_e\Gamma(1+z)}{4\pi d_L^2 m_e c^2} = (0.18 \text{ Jy}) \phi_f N_{e55} B \Gamma (1+z) d_{L28}^{-2}, \quad (2)$$

where  $d_L$  is the luminosity distance<sup>4</sup> to the source, and  $\phi_\nu$  and  $\phi_f$  are dimensionless constants that depend on the electron energy distribution index  $p$ ; for  $p = 5$  (as suggested by the high energy spectral index for GRB 080319B),  $\phi_\nu = 0.5$  and  $\phi_f = 0.7$  (cf. Wijers & Galama, 1999<sup>5</sup>). In all subsequent equations we explicitly use these values for the  $\phi$ 's with the exception that for the most important quantities – such as the total energy and the inverse Compton flux – we show the dependence of the results on the  $\phi$ 's to indicate how uncertainties in  $\nu_i$  and  $f_i$  affect the final result.

Throughout the paper we measure frequencies in eV and fluxes in Jy. All other quantities are in cgs units, but we use the short hand notation  $x_n \equiv x/(10^n \text{ cgs})$  to scale numerical

<sup>3</sup>Technically, the electron index  $p$  is a sixth parameter, but since it can be estimated directly from the high energy slope of the gamma-ray spectrum we do not count it

<sup>4</sup>The factor  $(1+z)$  in the numerator of the expression for flux, eq. 2, is due to the fact that the luminosity distance refers to the bolometric flux whereas we are considering the flux per unit frequency.

<sup>5</sup> $\phi_\nu = 1.5x_p$  and  $\phi_f = \phi_p$  in the notation of Wijers & Galama.

values, e.g.,  $R_{15} = R/(10^{15} \text{ cm})$  is the radius of the radiating shell with respect to the center of the explosion in units of  $10^{15} \text{ cm}$ . Using this convention, the source optical depth  $\tau_e$  and the duration of a pulse in the lightcurve  $\delta t$  (in seconds) are given by:

$$\tau_e = \frac{\sigma_T N_e}{4\pi R^2} = 0.5 \frac{N_{e55}}{R_{15}^2} \quad \text{or} \quad N_{e55} = 2\tau_e R_{15}^2, \quad (3)$$

$$\delta t = \frac{(1+z)R}{2c\Gamma^2} = (1.7 \times 10^4 \text{ s}) R_{15} \Gamma^{-2} (1+z). \quad (4)$$

Equivalently,

$$\Gamma = 130(\delta t)^{-1/2} (1+z)^{1/2} R_{15}^{1/2}. \quad (5)$$

We can combine equations (1) & (2) to eliminate  $B$ :

$$f_i = \frac{3 \times 10^7 \text{ Jy}}{\gamma_i^2} \nu_i N_{e55} (1+z)^2 d_{L28}^{-2}, \quad (6)$$

and use equation (3) to replace  $N_e$  by  $\tau_e$ . The resultant equation is:

$$f_i = \frac{4.2 \times 10^7 \text{ Jy}}{\gamma_i^4} \nu_i Y R_{15}^2 (1+z)^2 d_{L28}^{-2}, \quad (7)$$

or

$$\gamma_i = 81 f_i^{-1/4} \nu_i^{1/4} Y^{1/4} R_{15}^{1/2} (1+z)^{1/2} d_{L28}^{-1/2}. \quad (8)$$

Here we have defined the quantity

$$Y \equiv \gamma_i^2 \tau_e, \quad (9)$$

which is closely related to, but smaller by a factor of 2-3 compared with, the Compton-Y parameter for GRB 080319B (the difference depends on electron distribution function). Substituting eqs. (5) & (8) back into eq. (1), we find

$$B = (205G)(\delta t)^{1/2} \nu_i^{1/2} f_i^{1/2} Y^{-1/2} R_{15}^{-3/2} (1+z)^{-1/2} d_{L28}, \quad (10)$$

while equations (3) & (8) yield

$$N_{e55} = 2.9 \times 10^{-4} \nu_i^{-1/2} f_i^{1/2} Y^{1/2} R_{15} (1+z)^{-1} d_{L28}. \quad (11)$$

Equations (3), (5), (8), (10) and (11) are solutions for the five basic physical parameters of the synchrotron source in terms of the observed variability time  $\delta t$  and four unknown quantities: the source radius  $R_{15}$ , the Compton parameter  $Y$ , the peak energy of the synchrotron spectrum  $\nu_i$  and the synchrotron flux at the peak  $f_i$ . The last two quantities are not independent — they are constrained by the observed optical flux  $f_{op}$  ( $= 10 \text{ Jy}$  in the

case of GRB 080319B) at 2 eV. Depending on whether the synchrotron peak frequency  $\nu_i$  is below or above 2 eV, we obtain the following constraint:

$$f_{op} = \begin{cases} f_i(2/\nu_i)^{1/3}, & \nu_i > 2, \\ f_i(\nu_i/2)^{p/2}, & \nu_i < 2, \end{cases} \quad (12)$$

where we have used standard results for the spectral slope below and above the synchrotron peak, assuming for the latter that the cooling frequency is close to  $\nu_i$ , as suggested by the spectrum of GRB 080319B<sup>6</sup>; for other bursts, where the cooling break is substantially above the synchrotron peak, the equations in this paper can be easily modified by replacing  $p$  with  $(p - 1)$ .

Another constraint is provided by the synchrotron self-absorption frequency  $\nu_a$ , which can be estimated by equating the synchrotron flux at  $\nu_a$  to the blackbody flux in the Rayleigh-Jeans limit. Assuming that the electrons that dominate at  $\nu_a$  have Lorentz factor  $\gamma_i$ , we obtain

$$\frac{2\nu_a'^2}{c^2} m_e c^2 \gamma_i = f'(\nu_a') = \frac{f_i}{\Gamma} \frac{d_L^2}{(1+z)R^2} \left( \frac{\nu_a'}{\nu_i'} \right)^{1/3}, \quad (13)$$

where primes refer to quantities in the source comoving frame. To convert to the observer frame, we use

$$\nu_a \equiv \nu_a' \Gamma / (1+z). \quad (14)$$

Combining the above two equations we find

$$\nu_a = 3.8 f_i^{3/5} \nu_i^{-1/5} \Gamma^{3/5} \gamma_i^{-3/5} R_{15}^{-6/5} (1+z)^{-9/5} d_{L28}^{6/5}. \quad (15)$$

As before, all frequencies are in eV and fluxes in Jy. Substituting for  $\Gamma$  &  $\gamma_i$  from equations (5) and (8) results in

$$\nu_a = 5.1 f_i^{3/4} \nu_i^{-7/20} (\delta t)^{-3/10} R_{15}^{-6/5} Y^{-3/20} (1+z)^{-9/5} d_{L28}^{3/2}. \quad (16)$$

As we discuss in §3.2, we can estimate from the gamma-ray data the ratio  $\eta$  of the synchrotron frequency  $\nu_i$  to the self-absorption frequency  $\nu_a$ :

$$\eta \equiv \nu_i / \nu_a. \quad (17)$$

---

<sup>6</sup>The spectrum of GRB 080319B peaked at 650 keV and contained no other break between 20keV and 7 MeV. Since the cooling frequency cannot be smaller than 650 keV since the spectrum varies as  $\nu^{0.2}$  below the peak, it must be either larger than 7MeV or close to 650 keV. The former possibility is unlikely since it corresponds to a radiatively inefficient system and would increase the energy requirement of an already extreme burst.

Therefore, this is a third observational constraint on the source properties.

To summarize, the source of optical emission is described by means of five parameters. The pulse duration  $\delta t$ , the optical flux  $f_{op}$  and the frequency ratio  $\eta$  (eq. 17) give three constraints. The solution space is thus reduced to a two-dimensional surface. Additional constraints are obtained from the gamma-ray data, as we discuss next.

### 3.2. Gamma-ray emission via the inverse-Compton process

We assume that the gamma-rays are produced by inverse Compton (IC) scattering of synchrotron photons. The peak frequency  $\nu_{ic}$  of the IC spectrum and the flux  $f_{ic}$  at the peak are related to  $\nu_i$  and  $f_i$  as follows,

$$\nu_{ic} \approx 3\gamma_i^2 \nu_i, \quad f_{ic} \approx 3\tau_e f_i = 3Y \gamma_i^{-2} f_i, \quad (18)$$

where a multiplicative factor of 3 in the expression for  $f_{ic}$  takes into account the ratio of solid-angle integrated specific intensity inside the source and the flux just outside the shell (in the source comoving frame). Substituting for  $\gamma_i$  from equation (8),

$$\nu_{ic6} = 1.9 \times 10^{-2} f_i^{-1/2} \nu_i^{3/2} Y^{1/2} R_{15} (1+z) d_{L28}^{-1}, \quad (19)$$

$$f_{ic-3} = 0.47 f_i^{3/2} \nu_i^{-1/2} Y^{1/2} R_{15}^{-1} (1+z)^{-1} d_{L28}, \quad (20)$$

where  $\nu_{ic6} = \nu_{ic}/(10^6 \text{ eV})$  and  $f_{ic-3} = f_{ic}/(10^{-3} \text{ Jy})$ .

Using equation (19) for  $\nu_{ic}$  we determine the synchrotron peak flux,

$$f_i = 3.8 \times 10^{-4} \nu_{ic6}^{-2} \nu_i^3 R_{15}^2 Y (1+z)^2 d_{L28}^{-2}, \quad (21)$$

and substituting this into equation (16) we obtain  $\nu_i$ :

$$\nu_i = 1.2 \times 10^2 \eta^{-10/9} \nu_{ic6}^{5/3} (\delta t)^{1/3} R_{15}^{-1/3} Y^{-2/3} (1+z)^{1/3}. \quad (22)$$

Eliminating  $\nu_i$  from equation (21) by using eq. (22), we find

$$f_i = 6.6 \times 10^2 \eta^{-10/3} \nu_{ic6}^3 \delta t R_{15} Y^{-1} (1+z)^3 d_{L28}^{-2}. \quad (23)$$

Substituting for  $\nu_i$  and  $f_i$  from equations (22) & (23) into equation (12) for the optical flux we obtain

$$f_{op} = \begin{cases} 166 \eta^{-\frac{80}{27}} \nu_{ic6}^{\frac{22}{9}} (\delta t)^{\frac{8}{9}} R_{15}^{\frac{10}{9}} Y^{-\frac{7}{9}} (1+z)^{\frac{26}{9}} d_{L28}^{-2}, & \nu_i > 2, \\ 922 \times 8.7^p \eta^{-\frac{5(p+6)}{9}} \nu_{ic6}^{\frac{5p+18}{6}} (\delta t)^{\frac{p+6}{6}} R_{15}^{\frac{6-p}{6}} Y^{-\frac{p+3}{3}} (1+z)^{\frac{p+18}{6}} d_{L28}^{-2} (\phi_\nu/\phi_f)^{\frac{3+p}{3}}, & \nu_i < 2. \end{cases} \quad (24)$$



We use the optical flux to eliminate one more unknown variable,  $Y$ ,

$$Y = \begin{cases} 714 \eta^{-\frac{80}{21}} f_{op}^{-\frac{9}{7}} \nu_{ic6}^{\frac{22}{7}} (\delta t)^{\frac{8}{7}} R_{15}^{\frac{10}{7}} (1+z)^{\frac{26}{7}} d_{L28}^{-\frac{18}{7}}, & \nu_i > 2, \\ 471 \times 1.4^{\frac{3}{p+3}} \eta^{-\frac{5(p+6)}{3(p+3)}} f_{op}^{-\frac{3}{p+3}} \nu_{ic6}^{\frac{5p+18}{2p+6}} (\delta t)^{\frac{p+6}{2p+6}} R_{15}^{\frac{6-p}{2p+6}} (1+z)^{\frac{p+18}{2p+6}} d_{L28}^{-\frac{6}{p+3}}, & \nu_i < 2. \end{cases} \quad (25)$$

We are now in a position to express all quantities in terms of four observables, viz., the pulse duration  $\delta t$ , the optical flux  $f_{op}$ , the dimensionless self-absorption frequency  $\eta$ , and the peak frequency of the gamma-ray spectrum  $\nu_{ic}$ , plus one unknown parameter  $R_{15}$ .

The peak frequency of the synchrotron spectrum is obtained from equations (22) & (25):

$$\nu_i = \begin{cases} 1.5 \eta^{\frac{10}{7}} f_{op}^{\frac{6}{7}} \nu_{ic6}^{-\frac{3}{7}} (\delta t)^{-\frac{3}{7}} R_{15}^{-\frac{9}{7}} (1+z)^{-\frac{15}{7}} d_{L28}^{\frac{12}{7}}, & \nu_i > 2, \\ 2 \times 1.4^{-\frac{2}{p+3}} \eta^{\frac{10}{3(p+3)}} f_{op}^{\frac{2}{p+3}} \nu_{ic6}^{-\frac{1}{p+3}} (\delta t)^{-\frac{1}{p+3}} R_{15}^{-\frac{3}{p+3}} (1+z)^{-\frac{5}{p+3}} d_{L28}^{\frac{4}{p+3}}, & \nu_i < 2. \end{cases} \quad (26)$$

Let us define the transition radius  $R_{tr}$  as that value of  $R$  for which  $\nu_i = 2$  eV. From equation (26) we find

$$R_{tr,15} = 0.8 \eta^{\frac{10}{9}} f_{op}^{\frac{2}{9}} \nu_{ic6}^{-\frac{1}{3}} (\delta t)^{-\frac{1}{3}} (1+z)^{-\frac{5}{3}} d_{L28}^{\frac{4}{3}}. \quad (27)$$

Note that, for  $R > R_{tr}$ ,  $\nu_i < 2$  eV, and vice versa.

The flux at the peak of the synchrotron spectrum is obtained from eqs. (23) & (25):

$$f_i = \begin{cases} 0.92 \eta^{\frac{10}{21}} f_{op}^{\frac{9}{7}} \nu_{ic6}^{-\frac{1}{7}} (\delta t)^{-\frac{1}{7}} R_{15}^{-\frac{3}{7}} (1+z)^{-\frac{5}{7}} d_{L28}^{\frac{4}{7}}, & R < R_{tr}, \\ 1.4^{\frac{p}{p+3}} \eta^{-\frac{5p}{3(p+3)}} f_{op}^{\frac{3}{p+3}} \nu_{ic6}^{\frac{p}{2p+6}} (\delta t)^{\frac{p}{2p+6}} R_{15}^{\frac{3p}{2p+6}} (1+z)^{\frac{5p}{2p+6}} d_{L28}^{-\frac{2p}{p+3}}, & R > R_{tr}, \end{cases} \quad (28)$$

and the peak gamma-ray flux is obtained from equations (20), (25), (26) & (28):

$$f_{ic-3} = \frac{\phi_\nu}{\phi_f} \begin{cases} 12.3 \eta^{-\frac{40}{21}} f_{op}^{\frac{6}{7}} \nu_{ic6}^{\frac{11}{7}} (\delta t)^{\frac{4}{7}} R_{15}^{-\frac{2}{7}} (1+z)^{\frac{6}{7}} d_{L28}^{-\frac{2}{7}}, & R < R_{tr}, \\ 8.4 \times 1.4^{\frac{2p+4}{p+3}} \eta^{-\frac{10(p+2)}{3(p+3)}} f_{op}^{\frac{2}{p+3}} \nu_{ic6}^{\frac{2p+5}{p+3}} (\delta t)^{\frac{p+2}{p+3}} R_{15}^{\frac{p}{p+3}} (1+z)^{\frac{3p+4}{p+3}} d_{L28}^{-\frac{2p+2}{p+3}}, & R > R_{tr}. \end{cases} \quad (29)$$

Using equations (25), (26) & (28) to substitute for  $Y$ ,  $\nu_i$  &  $f_i$ , equations (8), (10) & (11) give

$$\gamma_i = \begin{cases} 555 \eta^{-\frac{5}{7}} f_{op}^{-\frac{3}{7}} \nu_{ic6}^{\frac{5}{7}} (\delta t)^{\frac{3}{14}} R_{15}^{\frac{9}{14}} (1+z)^{\frac{15}{14}} d_{L28}^{-\frac{6}{7}}, & R < R_{tr}, \\ 527 \eta^{-\frac{5}{3(p+3)}} f_{op}^{-\frac{1}{p+3}} \nu_{ic6}^{\frac{p+4}{2p+6}} (\delta t)^{\frac{1}{2p+6}} R_{15}^{\frac{3}{2p+6}} (1+z)^{\frac{5}{2p+6}} d_{L28}^{-\frac{4}{2(p+3)}}, & R > R_{tr}, \end{cases} \quad (30)$$

$$\begin{aligned}
 B = \phi_\nu^{-1} & \begin{cases} 4.5\text{G} \eta^{\frac{20}{7}} f_{op}^{\frac{12}{7}} \nu_{ic6}^{-\frac{13}{7}} (\delta t)^{-\frac{5}{14}} R_{15}^{-\frac{43}{14}} (1+z)^{-\frac{53}{14}} d_{L28}^{\frac{24}{7}}, & R < R_{tr}, \\ 6.7\text{G} \eta^{\frac{20}{3(p+3)}} f_{op}^{\frac{4}{p+3}} \nu_{ic6}^{-\frac{p+5}{p+3}} (\delta t)^{\frac{p-1}{2p+6}} R_{15}^{-\frac{p+15}{2p+6}} (1+z)^{-\frac{17-p}{2p+6}} d_{L28}^{\frac{8}{p+3}}, & R > R_{tr}, \end{cases} & (31) \\
 N_{e55} = & \begin{cases} 6.1 \times 10^{-3} \eta^{-\frac{50}{21}} f_{op}^{-\frac{3}{7}} \nu_{ic6}^{\frac{12}{7}} (\delta t)^{\frac{5}{7}} R_{15}^{\frac{15}{7}} (1+z)^{\frac{11}{7}} d_{L28}^{-\frac{6}{7}}, & R < R_{tr}, \\ 5.9 \times 10^{-3} \eta^{-\frac{5(p+4)}{3(p+3)}} f_{op}^{-\frac{1}{p+3}} \nu_{ic6}^{\frac{3p+10}{2p+6}} (\delta t)^{\frac{p+4}{2p+6}} R_{15}^{\frac{3p+12}{2p+6}} (1+z)^{\frac{p+8}{2p+6}} d_{L28}^{-\frac{2}{p+3}}, & R > R_{tr}. \end{cases} & (32)
 \end{aligned}$$

The energy in the magnetic field as measured in the GRB host galaxy rest frame is  $E_B = B^2 R^3/2$ . Using equation (31), this can be shown to be

$$E_B = \begin{cases} 1.2 \times 10^{46} \text{erg} \eta^{\frac{40}{7}} f_{op}^{\frac{24}{7}} \nu_{ic6}^{-\frac{26}{7}} (\delta t)^{-\frac{5}{7}} R_{15}^{-\frac{22}{7}} (1+z)^{-\frac{53}{7}} d_{L28}^{\frac{48}{7}} \phi_\nu^{-2}, & R < R_{tr}, \\ 2 \times 10^{46} \text{erg} \eta^{\frac{40}{3(p+3)}} f_{op}^{\frac{8}{p+3}} \nu_{ic6}^{-\frac{2p+10}{p+3}} (\delta t)^{\frac{p-1}{p+3}} R_{15}^{\frac{2p-6}{p+3}} (1+z)^{-\frac{17-p}{p+3}} d_{L28}^{\frac{16}{p+3}} \phi_\nu^{-2}, & R > R_{tr}. \end{cases} \quad (33)$$

The energy in the charged particles ( $e^\pm$ ) that produce the optical and gamma-ray emission is  $E_e = N_e \gamma_i \Gamma m_e c^2$ . From equations (5), (30) & (32) this is

$$E_e = \begin{cases} 4 \times 10^{51} \text{erg} \eta^{-\frac{65}{21}} f_{op}^{-\frac{6}{7}} \nu_{ic6}^{\frac{17}{7}} (\delta t)^{\frac{3}{7}} R_{15}^{\frac{23}{7}} (1+z)^{\frac{22}{7}} d_{L28}^{-\frac{12}{7}} (\phi_\nu/\phi_f)^{\frac{1}{2}}, & R < R_{tr}, \\ 3 \times 10^{51} \text{erg} \eta^{-\frac{(5p+25)}{3(p+3)}} f_{op}^{-\frac{2}{p+3}} \nu_{ic6}^{\frac{2p+7}{p+3}} (\delta t)^{\frac{1}{p+3}} R_{15}^{\frac{2p+9}{p+3}} (1+z)^{\frac{p+8}{p+3}} d_{L28}^{-\frac{4}{p+3}} (\phi_\nu/\phi_f)^{\frac{1}{2}}, & R > R_{tr}. \end{cases} \quad (34)$$

We should also consider the energy in the protons arising from the bulk relativistic motion of the shell. However, to estimate this quantity we need to make some assumption regarding the composition of the fluid in the shell, whether it is primarily an  $e^+e^-$  plasma or a  $p^+e^-$  plasma. In the former case the energy in protons is negligible, while in the latter case the energy is  $E_p = N_e \Gamma m_p c^2 \sim \text{few} \times E_e$  (taking  $\gamma_i$  of order a few hundred).

In the observer frame, the synchrotron cooling time  $t_{syn}$  is

$$t_{syn} = (7.7 \times 10^8 \text{s}) (1+z) \Gamma^{-1} B^{-2} \gamma_i^{-1}, \quad (35)$$

which, using equations (5), (30) and (31), can be written as

$$t_{syn} = \frac{\phi_\nu^{5/2}}{\phi_f^{1/2}} \begin{cases} (620\text{s}) \eta^{-5} f_{op}^{-3} \nu_{ic6}^3 (\delta t) R_{15}^5 (1+z)^7 d_{L28}^{-6}, & R < R_{tr}, \\ (295\text{s}) \eta^{-\frac{35}{3(p+3)}} f_{op}^{-\frac{7}{p+3}} \nu_{ic6}^{\frac{3p+16}{2p+6}} (\delta t)^{\frac{4-p}{2p+6}} R_{15}^{\frac{p+24}{2p+6}} (1+z)^{\frac{32-p}{2p+6}} d_{L28}^{-\frac{14}{p+3}}, & R > R_{tr}. \end{cases} \quad (36)$$

In addition to the loss of energy via synchrotron radiation, electrons also lose energy through IC scattering of the local radiation field. We calculate the photon energy density in the source rest frame from the observed bolometric luminosity  $L_{obs}$ , and use this to estimate the IC cooling time  $t_{ic}$  in the observer frame:

$$t_{ic} = \frac{4\pi R^2 \Gamma(1+z) m_e c^2}{L_{obs} \gamma_i \sigma_T} = (0.2\text{s}) L_{obs,52}^{-1} (\delta t)^{-1/2} R_{15}^{5/2} (1+z)^{3/2} \gamma_i^{-1}. \quad (37)$$

Strictly speaking we do not know the true bolometric luminosity, so the above estimate of  $t_{ic}$  is an upper limit to the actual inverse-Compton cooling time. Using equation (30) we can rewrite  $t_{ic}$  in the following more useful form:

$$t_{ic} = \frac{\phi_\nu^{1/2}}{\phi_f^{1/2}} \begin{cases} \frac{4 \times 10^{-4} \text{s}}{L_{obs,52}} \eta^{5/7} f_{op}^{3/7} \nu_{ic6}^{-5/7} (\delta t)^{-5/7} R_{15}^{13/7} (1+z)^{3/7} d_{L28}^{6/7}, & R < R_{tr}, \\ \frac{4.5 \times 10^{-4} \text{s}}{L_{obs,52}} \eta^{5/(p+3)} f_{op}^{1/p+3} \nu_{ic6}^{-p+4} (\delta t)^{-p+4/2p+6} R_{15}^{5p+12/2p+6} (1+z)^{3p+4/2p+6} d_{L28}^{2/p+3}, & R > R_{tr}. \end{cases} \quad (38)$$

All the results obtained so far are general and could be applied to any GRB that has the required data. We now consider the implications for the naked eye burst GRB 080319B.

#### 4. Application to GRB 080319B: Ruling out the internal shock model

The relevant observational parameters for GRB 080319B are:  $z = 0.94$ ,  $d_{L28} = 1.9$ ,  $f_{op} = 10$  Jy,  $\nu_{ic6} = 0.665$ ,  $p = 5$ , and  $\delta t \sim 1$  s (from the gamma-ray variability). Moreover, we estimate that<sup>7</sup> the time-averaged  $\eta \equiv \nu_i/\nu_a$  for this burst was about 25 (because  $f_\nu \propto \nu^{0.18 \pm 0.01}$  between 20keV and 650 keV), whereas the initial value of  $\eta$  was  $\sim 10$  as  $f_\nu \propto \nu^{0.5 \pm 0.04}$  during the first 8 s. Scaling all quantities to these values, the transition radius  $R_{tr}$  becomes

$$R_{tr,16} = 12 \eta_{1.4}^{10/9} f_{op,1}^{2/3} \nu_{ic5.8}^{-1/3} (\delta t)^{-1/3}. \quad (39)$$

If  $R_{16} > R_{tr,16}$ , then  $\nu_i < 2$  eV and the optical band is in the steep decaying part of the synchrotron spectrum, above the synchrotron peak. If  $R_{16} < R_{tr,16}$ , then the synchrotron

---

<sup>7</sup>The spectral indices are obtained by fitting the data with the Band function, which gives the asymptotic value for the low energy and high energy index. It should be noted that the IC spectrum below  $\sim 2\gamma_i^2\nu_a$  is  $f_\nu \propto \nu$  and between this frequency and the peak of  $\nu f_\nu$  at  $3\gamma_i^2\nu_i$  the spectrum changes from  $f_\nu \propto \nu$  to  $\nu^{-1}$ . Therefore, somewhere in between these two frequencies the index would be 0.2. The Konus data for GRB 080319B found the spectral peak to be at 665 keV and the observations extended down to a minimum photon energy of 20 keV. Therefore, the IC spectral index of 0.2 at 20 keV requires  $\nu_i/\nu_a \sim 25$ .

peak is above 2 eV, and the optical band is in the  $F_\nu \propto \nu^{1/3}$  part of the synchrotron spectrum. Since the prompt optical emission in GRB 080319B was exceptionally bright, it is likely that the peak of the synchrotron spectrum was fairly close to the optical band. This suggests that  $R_{16}$  must be within a factor of a few of  $R_{tr,16}$ . According to equation (39),  $R_{tr} \sim 10^{17}$  cm, which is orders of magnitude larger than the radius at which internal shocks are expected. In fact, it is comparable to the deceleration radius of the jet.

From the results described in §3, we obtain the following numerical results for the relevant parameters in GRB 080319B:

$$\Gamma = 572(\delta t)^{-1/2} R_{16}^{1/2}, \quad (40)$$

$$\gamma_i = \begin{cases} 77 \eta_{1.4}^{-\frac{5}{7}} f_{op,1}^{-\frac{3}{7}} \nu_{ic5.8}^{\frac{5}{7}} (\delta t)^{\frac{3}{14}} R_{16}^{\frac{9}{14}}, & R < R_{tr}, \\ 251 \eta_{1.4}^{-\frac{5}{24}} f_{op,1}^{-\frac{1}{8}} \nu_{ic5.8}^{\frac{9}{16}} (\delta t)^{\frac{1}{16}} R_{16}^{\frac{3}{16}}, & R > R_{tr}, \end{cases} \quad (41)$$

$$N_e = \begin{cases} (1.1 \times 10^{51}) \eta_{1.4}^{-\frac{50}{21}} f_{op,1}^{-\frac{3}{7}} \nu_{ic5.8}^{\frac{12}{7}} (\delta t)^{\frac{5}{7}} R_{16}^{\frac{15}{7}}, & R < R_{tr}, \\ (3.4 \times 10^{51}) \eta_{1.4}^{-\frac{15}{8}} f_{op,1}^{-\frac{1}{8}} \nu_{ic5.8}^{\frac{25}{16}} (\delta t)^{\frac{9}{16}} R_{16}^{\frac{27}{16}}, & R > R_{tr}, \end{cases} \quad (42)$$

$$Y = \begin{cases} 2.5 \times 10^{-3} \eta_{1.4}^{-\frac{80}{21}} f_{op,1}^{-\frac{9}{7}} \nu_{ic5.8}^{\frac{22}{7}} (\delta t)^{\frac{8}{7}} R_{16}^{\frac{10}{7}}, & R < R_{tr}, \\ 7.5 \times 10^{-2} \eta_{1.4}^{-\frac{55}{24}} f_{op,1}^{-\frac{3}{8}} \nu_{ic5.8}^{\frac{43}{16}} (\delta t)^{\frac{11}{16}} R_{16}^{\frac{1}{16}}, & R > R_{tr}. \end{cases} \quad (43)$$

$$E_B = \begin{cases} (2 \times 10^{55} \text{erg}) \eta_{1.4}^{\frac{40}{7}} f_{op,1}^{\frac{24}{7}} \nu_{ic5.8}^{-\frac{26}{7}} (\delta t)^{-\frac{5}{7}} R_{16}^{-\frac{22}{7}}, & R < R_{tr}, \\ (2.3 \times 10^{51} \text{erg}) \eta_{1.4}^{\frac{5}{3}} f_{op,1} \nu_{ic5.8}^{-\frac{5}{2}} (\delta t)^{\frac{1}{2}} R_{16}^{\frac{1}{2}}, & R > R_{tr}, \end{cases} \quad (44)$$

$$E_e = \begin{cases} (3.4 \times 10^{49} \text{erg}) \eta_{1.4}^{-\frac{65}{21}} f_{op,1}^{-\frac{6}{7}} \nu_{ic5.8}^{\frac{17}{7}} (\delta t)^{\frac{3}{7}} R_{16}^{\frac{23}{7}}, & R < R_{tr}, \\ (3.3 \times 10^{50} \text{erg}) \eta_{1.4}^{-\frac{50}{24}} f_{op,1}^{-\frac{1}{4}} \nu_{ic5.8}^{\frac{17}{8}} (\delta t)^{\frac{1}{8}} R_{16}^{\frac{19}{8}}, & R > R_{tr}, \end{cases} \quad (45)$$

$$t_{syn} = \begin{cases} (7.4 \times 10^{-4} \text{s}) \eta_{1.4}^{-5} f_{op,1}^{-3} \nu_{ic5.8}^3 (\delta t) R_{16}^5, & R < R_{tr}, \\ (2 \text{s}) \eta_{1.4}^{-\frac{35}{24}} f_{op,1}^{-\frac{7}{8}} \nu_{ic5.8}^{\frac{31}{16}} (\delta t)^{\frac{1}{16}} R_{16}^{\frac{29}{16}}, & R > R_{tr}, \end{cases} \quad (46)$$

$$t_{ic} = \begin{cases} \frac{2.1 \text{s}}{L_{obs,52}} \eta_{1.4}^{\frac{5}{7}} f_{op,1}^{\frac{3}{7}} \nu_{ic5.8}^{-\frac{5}{7}} (\delta t)^{-\frac{5}{7}} R_{16}^{\frac{13}{7}}, & R < R_{tr}, \\ \frac{0.7 \text{s}}{L_{obs,52}} \eta_{1.4}^{\frac{5}{24}} f_{op,1}^{\frac{1}{8}} \nu_{ic5.8}^{-\frac{9}{16}} (\delta t)^{-\frac{9}{16}} R_{16}^{\frac{37}{16}}, & R > R_{tr}, \end{cases} \quad (47)$$

$$f_{ic-3} = \begin{cases} 7.1 \times 10^{-2} \eta_{1.4}^{-\frac{40}{21}} f_{op,1}^{\frac{6}{7}} \nu_{ic5.8}^{\frac{11}{7}} (\delta t)^{\frac{4}{7}} R_{16}^{-\frac{2}{7}}, & R < R_{tr}, \\ 7.8 \times 10^{-3} \eta_{1.4}^{-\frac{35}{12}} f_{op,1}^{\frac{1}{4}} \nu_{ic5.8}^{\frac{15}{8}} (\delta t)^{\frac{7}{8}} R_{16}^{\frac{5}{8}}, & R > R_{tr}. \end{cases} \quad (48)$$

Figure 1 shows the dependences of a number of quantities as functions of the only free parameter in the model:  $R_{16}$ . The lower solid line in the top left panel shows the predicted gamma-ray flux  $f_{ic-3}$  (based on eq. 48) and immediately indicates a major problem. If, as we suggested earlier,  $R_{16} \sim R_{tr,16}$ , then the peak IC flux  $f_{ic}$  that the model predicts falls short of the observed flux by nearly a factor of 100

In Appendix A we discuss possible sources of error in our estimate of the IC flux. We show that the uncertainty in  $f_{ic}$ , even after allowing for inhomogeneities in the source, is no larger than a factor of order unity. The largest error is that we have overestimated  $\nu_a$  by a factor  $\sim 1.5$  by not including the expansion of the source during the time it takes for a photon to cross the shell (see Appendix A). The effect of this is that  $f_{ic}$  is underestimated by a factor  $\sim 2.5$  due to its dependence on  $\nu_a$  via  $\eta$ . Even after correcting for this (upper solid line in upper left panel in Fig. 1), the theoretically calculated gamma-ray flux is still smaller than the observed value by a factor  $\sim 30$ . This discrepancy is much too large to be overcome by minor adjustments to the model. We thus conclude that the internal shock model with  $R_{16} \sim R_{tr,16}$  is ruled out for GRB 080319B.

One way to mitigate this problem is to select values of  $R_{16}$  that are either very much smaller or very much larger than  $R_{tr,16}$ . However, as Fig. 1 shows, we need to modify  $R_{16}$  by a huge factor, which immediately leads to other problems.

The top right panel indicates one of the problems we face. This panel shows the total isotropic energy of the source ( $E_B + E_e$ ) in units of  $10^{55}$  erg. We see that shifting  $R_{16}$  substantially away from  $R_{tr,16}$  causes the total energy to become unphysically large. A reasonable upper limit to the total energy is  $10^{55}$  erg<sup>8</sup>, which corresponds to an energy of  $\sim 2 \times 10^{53}$  erg in each spike in the gamma-ray lightcurve. The energy estimates in equations (44) and (45) refer to the latter and the limit is shown by the dotted line in the top right panel. We see that the energy constraint restricts  $R_{16}$  to lie within the range 4.4 – 14.6. Within this range of  $R_{16}$ , we have approximate equipartition between  $E_B$  and  $E_e$  (see the dashed line), which is desirable, whereas choosing other values of  $R_{16}$  would cause large deviations from equipartition.

---

<sup>8</sup>The isotropic energy release for GRB 080319B in the 20 keV – 7 MeV band was  $1.3 \times 10^{54}$  erg. The radiative efficiency for GRBs varies widely from burst to burst but is generally larger than  $\sim 10\%$  (Panaitescu & Kumar, 2002). Therefore, the total energy release in GRB 080319B is expected to be  $\lesssim 1.3 \times 10^{55}$  erg, and so we take  $(E_B + E_e) \lesssim 10^{55}$ .

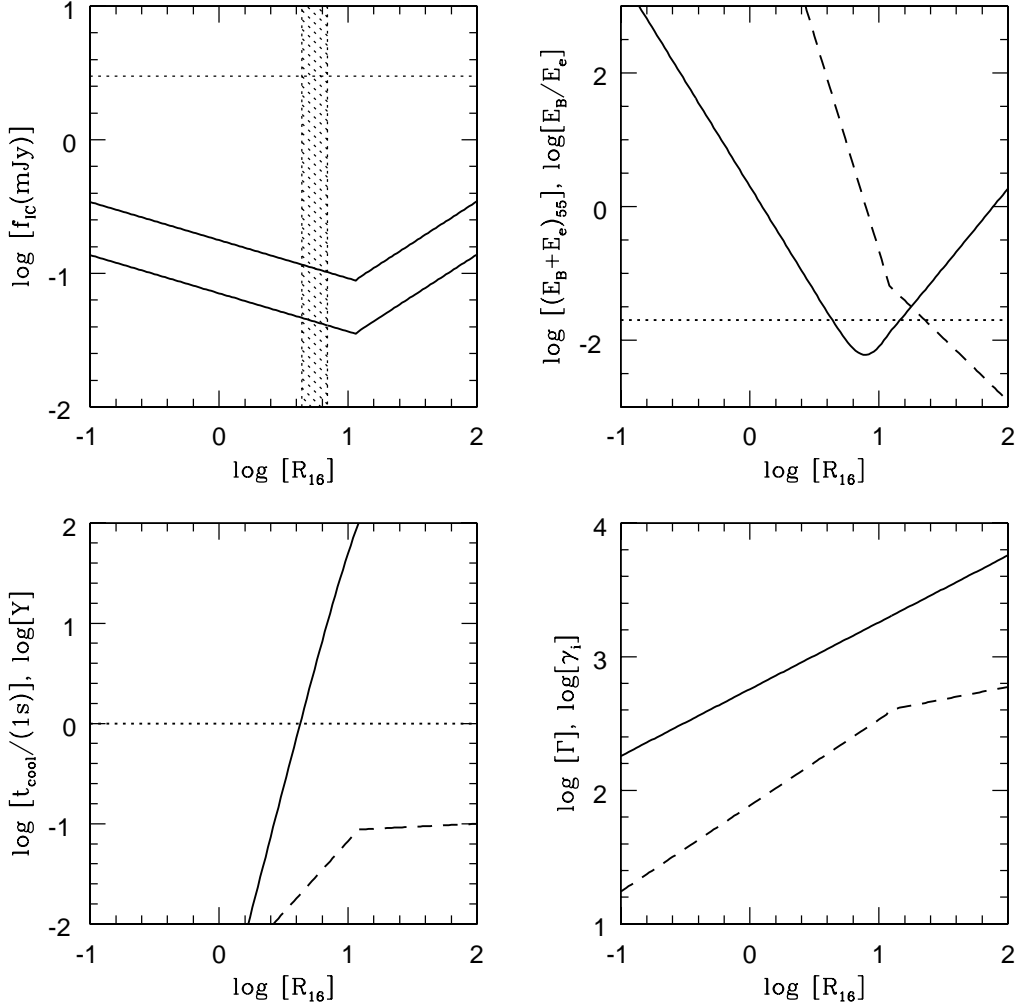


Fig. 1.— Top left: Shows the IC flux in GRB 080319B at 650 keV predicted by the internal shock model. The lower line is from eq. (48) and the upper line corresponds to a factor of 2.5 larger flux to allow for the expansion of the source during a photon crossing time, which was not included in calculations presented in §3 and §4 (see the Appendix for details and for a discussion of uncertainties in  $f_{ic}$  and  $\nu_a$ ). The shaded band is the region of the source radius  $R_{16}$  that is favored by various constraints (see text for details). For these values of  $R_{16}$ , the predicted IC flux falls short of the observed gamma-ray flux (horizontal dotted line) by a factor  $\gtrsim 30$ . Top right: The solid line shows the total isotropic energy in a single variability spike in the gamma-ray lightcurve. The dotted line shows the maximum energy allowed. The dashed line shows  $E_B/E_e$ . Bottom left: The solid line shows the cooling time in units of the variability time (1s) – which should be  $\gtrsim 1$  since the low energy spectral index was positive – and the dashed line shows the Compton  $Y$ . Bottom right: The solid line shows the bulk Lorentz factor  $\Gamma$  and the dashed line shows the typical Lorentz factor of electrons  $\gamma_i$ .

The bottom left panel in Fig. 1 shows another set of problems. Given the huge luminosity of GRB 080319B, we expect the source to be radiatively efficient, which means that  $t_{\text{cool}}$  must be comparable to the variability time  $t_{\text{var}} \sim \delta t \sim 1$  s. We see that the cooling time  $t_{\text{cool}}$ , calculated according to

$$\frac{1}{t_{\text{cool}}} = \frac{1}{t_{\text{syn}}} + \frac{1}{t_{\text{ic}}}, \quad (49)$$

is within a factor of 10 of the variability time only for models with  $R_{16}$  in the narrow range 2.7 – 6.9. (The variation of  $t_{\text{cool}}$  with  $R_{16}$  is extremely steep, so the condition  $t_{\text{cool}} \sim t_{\text{var}}$  is very restrictive.) Combining this constraint with the one we obtained earlier from the total energy, the allowed range of  $R_{16}$  is limited to 4.4 – 6.9, shown as the hatched vertical band in the top left panel in Fig. 1. We also see from the bottom left panel that the Compton  $Y$  is less than 0.1 for most models, and extremely small,  $Y \ll 0.1$ , for small values of  $R_{16}$ . Since  $Y$  determines the fraction of the source luminosity that comes out in gamma-rays, and since GRB 080319B (indeed, any GRB) is a strong gamma-ray source, it seems unlikely that  $Y$  could be this small.

Finally, the bottom right panel in Fig. 1 shows the dependence of the bulk Lorentz factor  $\Gamma$  and the random electron Lorentz factor  $\gamma_i$  on  $R_{16}$ . Models with  $R_{16} \sim R_{tr,16}$  predict reasonable values  $\sim 10^2 - 10^3$  for both Lorentz factors, but models with very different values of  $R_{16}$  predict either unusually low or unusually high values.

In summary, all the indications suggest that the optical and gamma-ray radiation in GRB 080319B were produced at a radius  $R \sim \text{few} \times 10^{16} \text{ cm} - 10^{17} \text{ cm}$ . But at this radius, the internal shock model predicts a negligibly small gamma-ray flux. We are thus forced to conclude that the internal shock model, at least in its standard form, is definitely ruled out for GRB 080319B.

#### 4.1. Other versions of the internal shock model

We now consider whether we can get around the above difficulty by modifying the internal shock model. We begin by noting that, as long as the gamma-ray emission is IC – something that is required by the low energy spectrum  $f_\nu \propto \nu^{0.5}$  at early times (§2) – and the seed synchrotron photons are produced in the same source as the  $\gamma$ -ray photons, equation (48) is valid. This equation predicts an unacceptably low flux in the gamma-ray band. Therefore, if we wish to save the internal shock model, we must give up the assumption that all the radiation came from the same region of the source.

Let us assume that the seed photons for IC scattering are produced by the same source that gave us the optical flash. We will call this the *optical region* of the source. Let us

assume that these seed photons are IC-scattered in a different region, the *gamma-ray region*. We now show that the electron Lorentz factors  $\gamma_i$  in two regions are very similar.

Let us suppose that  $\gamma_i$  in the optical region differs from that in the gamma-ray region. Then, the self-IC radiation from the optical region will introduce a second IC component in the observed spectrum, with a peak at a different photon energy. Equation (48) is valid for any SSC process, so we can use it to estimate the flux in the second peak. If the IC peak from the optical region is at a higher photon energy than 650 keV by a factor  $> 2.5$ , then equation (48) shows that the flux in this component will be larger than the observed flux (note that  $f_{ic} \propto \nu_{ic}^{11/7}$  as per eq. 48, and the observed flux above 650 keV declined as  $\nu^{-2.87}$ ). On the other hand, if the self-IC radiation peaks at an energy much less than 650 keV, the magnetic energy in the source will increase very rapidly ( $E_B \propto \nu_{ic}^{-26/7}$ , eq. 44). Since the energy is already close to the maximum limiting value we can accept, this option is also ruled out.

Therefore, the values of  $\gamma_i$  in the optical and gamma-ray regions must be nearly the same. This tight relation between the Lorentz factors in the two regions suggests that the optical and gamma-ray sources are very likely the same region. Even if they are not, the similarity of their parameters means that the large discrepancy in the gamma-ray flux discussed previously will survive unchanged. A related idea is that there are two populations of electrons with different values of  $\gamma_i$  within the same source. One population is responsible for the seed photons and the other for the IC scattering. This possibility can be ruled out by the same argument.

This leads us to consider a model in which part of a shell is magnetized – this is where optical photons are produced – and the rest has a much weaker magnetic field (in order to avoid overproducing synchrotron flux) but contains about 30 times more electrons in order to produce the observed  $\sim 3\text{mJy}$   $\gamma$ -ray flux via IC scattering. This situation can arise, for instance, when magnetic field decays downstream of a shock front, as suggested in Kumar & Panaitescu (2008). However, this proposal suffers from serious problems that these authors have pointed out in their paper. The solution requires magnetic field to decay on a length scale that is about 5% of the shell thickness or about  $10^7$  plasma skin depth. This scale corresponds to no particular physical scale in the system and is quite arbitrary. An even more severe problem is that the model cannot account for the shorter time scale variability of gamma-rays compared to the optical; in fact, the natural expectation is the opposite in this model.

Note that Fig. 1 indicates an extremely narrow range of  $R$  for the radiating medium. It is hard to believe that a large number of independent shells ejected from the central source would all collide at exactly this radius. In addition, as we noted earlier, the radius  $R$  of the



source is uncomfortably large for the internal shock model. Both of these features would be explained naturally if we assumed that the internal shocks are not between independent shells, but rather between successive shells and the outermost shell, which is decelerating after colliding with the external medium. This is a variation on the general idea of internal shocks (with a strong hint of the forward shock model, see §5.2.2), which at least provides an explanation for the radius of the source. However, this model can be ruled out for two reasons. As with all other variants, this model cannot explain the magnitude of the IC flux unless the magnetic field occupies a small fraction of the shocked shell, about 5% of the ejecta width or  $10^7$  plasma skin depths. Furthermore, it predicts that the pulse-width should increase with time, which is inconsistent with the observed data for GRB 080319B which show, if anything, that the last few pulses in the gamma-ray lightcurve were somewhat narrower than the initial few pulses.

Having considered these and other ideas, we believe that it is impossible to explain the observations of GRB 080319B with any reasonable version of the internal shock model. Fortunately, there is an alternative model which invokes relativistic turbulence in the radiating fluid. We now apply this model to GRB 080319B.

## 5. Relativistic turbulence model for GRB 080319B

The basic kinematic features of the relativistic turbulence model are described in Narayan & Kumar (2008). In brief, this model explains the observed variability in GRB lightcurves by postulating an inhomogeneous relativistic velocity field in the GRB-producing medium (which we refer to as the “shell” because of its shell-like morphology in the host galaxy frame). The beaming effect of the turbulent eddies causes large amplitude fluctuations in the observed flux. Despite being inhomogeneous, the model is radiatively efficient in the sense that the whole medium radiates and the observer receives a fair share of the radiated luminosity. This important feature, which is a direct consequence of beaming, allows the model to overcome the arguments of Sari & Piran (1997) against inhomogeneous GRB models. The reader is referred to Narayan & Kumar (2008) for details.

Since the relativistic turbulence model has a natural explanation for the observed variability, equation (4) relating the variability time scale  $\delta t$  to  $R$  and  $\Gamma$  is no longer needed. Instead, the quantity  $R/2\Gamma^2c$  determines the *total* burst duration  $t_\gamma$ . We thus have

$$t_\gamma \sim \frac{R(1+z)}{2c\Gamma^2} = (1.7 \times 10^4 \text{ s})R_{15}\Gamma^{-2}(1+z). \quad (50)$$

Since  $t_\gamma \sim 50$  s for GRB 080319B, whereas  $\delta t \sim t_{var} \sim 1$  s, this modification has a rather profound effect on the results.

In the relativistic turbulent model, we consider turbulent eddies with a typical bulk Lorentz factor  $\gamma_t$  in the frame of the shell, and a typical size  $\sim R/(\gamma_t\Gamma)$  in the comoving frame of an eddy. The eddies are volume-filling, so there are  $\sim \gamma_t^3$  eddies in a causally connected region of volume  $\sim R^3/\Gamma^3$ . We assume that the velocity field of eddies changes direction by  $\sim 2\pi$  on the light crossing time scale  $\sim R/(c\gamma_t\Gamma)$ . In this case the probability that an eddy, some time during its life, will move towards the observer with a velocity vector within an angle  $(\gamma_t\Gamma)^{-1}$  of the line-of-sight is  $\sim \gamma_t^{-1}$  (Narayan & Kumar, 2008). Therefore, over the course of the burst, a given observer will receive emission from  $\gamma_t^2$  eddies, with each eddy producing a pulse of radiation lasting a time (see Narayan & Kumar 2008 for details).

$$t_{var} \sim t_\gamma/\gamma_t^2. \quad (51)$$

Since GRB 080319 has  $t_{var} \sim t_\gamma/100$ , we infer that  $\gamma_t \sim 10$  for this burst. Note that, at any given time, the observer receives radiation from only one eddy on average.

We assume that the fluid in the shell consists of eddies and an inter-eddy medium. The latter is produced when eddies collide and shock. Let us take the thermal Lorentz factor of electrons within an eddy to be  $\gamma_{it}$ . The thermal Lorentz factor of electrons in the inter-eddy medium follows from energy conservation when eddies collide, and is  $\sim \gamma_{it}\gamma_t \equiv \gamma_i$ . Similarly, if we take the magnetic field in the inter-eddy frame to be  $B$ , then the comoving magnetic field in an eddy is  $B/\gamma_t^{1/2}$ , assuming that the magnetic energy is roughly conserved when eddies dissipate. Using these scalings we see that the peak of the synchrotron spectrum (as measured in the shell frame) for inter-eddy and eddy emissions are proportional to  $B\gamma_i^2$  and  $B\gamma_i^2\gamma_t^{-3/2}$ , respectively.

Let us take the average number of electrons in an eddy to be  $N_{ed}$ , and the total number of electrons in the inter-eddy medium in a volume  $(R/\Gamma)^3$  (the volume of a causally connected region) to be  $N_i$ . For simplicity, let us assume that the total number of electrons in all the  $\gamma_t^3$  eddies is of order  $N_i$ , i.e., half of the fluid in the shell is in eddies and the other half is in the inter-eddy medium. Thus we have  $N_{ed} \sim N_i/\gamma_t^3$ .

At any given time, only one eddy will produce beamed radiation towards the observer. The peak synchrotron flux from this eddy is proportional to  $\sim BN_{ed}\gamma_t^{3/2}\Gamma^3 \sim BN_i\Gamma^3/\gamma_t^{3/2}$ . Here we have made use of the fact that, at a fixed observer time, the observer receives radiation from only a fraction of the electrons in the eddy,  $\sim N_e/\gamma_t$ , due to the time dependence of eddy velocity direction. The peak synchrotron flux from the inter-eddy medium is  $\sim BN_i\Gamma^3$ , which is larger than the peak flux from the eddy by a factor  $\sim \gamma_t^{3/2}$ . The synchrotron flux in a fixed observer band above the peak frequency is larger for the inter-eddy medium by an additional factor of  $\gamma_t^{3(p-1)/4}$ . We thus conclude that the synchrotron emission observed in the optical band is completely dominated by the inter-eddy medium. We therefore ignore eddies when we estimate the optical synchrotron flux.

The situation is different for the IC emission. Let us write the synchrotron flux as seen by a typical electron in the inter-eddy medium as  $f_{syn}$  (this is easily estimated from the calculation above). The observed IC luminosity due to electrons in the inter-eddy medium  $f_{ic}^{ie}$  is then

$$f_{ic}^{ie} \propto \sigma_T f_{syn} N_i \Gamma^3, \quad (52)$$

while the IC emission from an eddy pointing towards the observer  $f_{ic}^{eddy}$  is

$$f_{ic}^{eddy} \propto \sigma_T (\gamma_t f_{syn}) N_{ed} (\Gamma \gamma_t)^3 / \gamma_t \sim \sigma_T f_{syn} N_i \Gamma^3 \quad (53)$$

We see that the two contributions are equal. Therefore, both components in the shell fluid contribute equally to the gamma-ray IC flux. Of course, the inter-eddy contribution will vary smoothly over the duration of the burst, whereas the contribution from the eddies will be highly variable.

Using these results, we may easily estimate the values of various parameters in GRB 080319B corresponding to the relativistic turbulence model. Note that, since the synchrotron radiation, or optical flux, comes from the inter-eddy plasma, it satisfies the same equations as derived in §4. Moreover, the IC flux has no dependence on the Lorentz factor of turbulent eddies (eq. 53). Therefore, equations (39)–(48) may be directly used for the relativistic turbulence model provided we replace  $\delta t$  with the burst duration 50 s, and take  $N_e$ ,  $E_B$ ,  $E_e$  and  $f_{ic}$  to be two times larger than the values given by these equations (the factor of two is to count both the eddies and the inter-eddy medium).

Setting  $\delta t = 50$  s (eq. 50),  $f_{op} = 10$  Jy,  $\nu_{ic} = 650$  keV and  $\eta_{1.4} = 1$  (i.e.,  $\eta = \nu_i / \nu_a \approx 25$ ) into equation (39) we obtain the transition radius

$$R_{tr} = 2 \times 10^{16} \text{ cm}. \quad (54)$$

The other parameters follow from equations (40)–(48)

$$\Gamma = 81 R_{16}^{1/2}, \quad (55)$$

$$\gamma_i = \begin{cases} 254 R_{16}^{9/14}, & R < R_{tr}, \\ 349 R_{16}^{3/16}, & R > R_{tr}, \end{cases} \quad (56)$$

$$N_e = \begin{cases} 9.4 \times 10^{52} R_{16}^{15/7}, & R < R_{tr}, \\ 1.3 \times 10^{53} R_{16}^{27/16}, & R > R_{tr}, \end{cases} \quad (57)$$

$$Y = \begin{cases} 2.1 R_{16}^{\frac{10}{7}}, & R < R_{tr}, \\ 5.5 R_{16}^{\frac{1}{16}}, & R > R_{tr}, \end{cases} \quad (58)$$

$$E_B = \begin{cases} (2.6 \times 10^{53} \text{erg}) R_{16}^{-\frac{22}{7}}, & R < R_{tr}, \\ (1.9 \times 10^{52} \text{erg}) R_{16}^{\frac{1}{2}}, & R > R_{tr}, \end{cases} \quad (59)$$

$$E_e = \begin{cases} (1.3 \times 10^{51} \text{erg}) R_{16}^{\frac{23}{7}}, & R < R_{tr}, \\ (2.6 \times 10^{51} \text{erg}) R_{16}^{\frac{19}{8}}, & R > R_{tr}, \end{cases} \quad (60)$$

$$t_{syn} = \begin{cases} (0.3\text{s}) R_{16}^5, & R < R_{tr}, \\ (2.8\text{s}) R_{16}^{\frac{29}{16}}, & R > R_{tr}, \end{cases} \quad (61)$$

$$t_{ic} = \begin{cases} \frac{0.1\text{s}}{L_{obs,52}} R_{16}^{\frac{13}{7}}, & R < R_{tr}, \\ \frac{0.07\text{s}}{L_{obs,52}} R_{16}^{\frac{37}{16}}, & R > R_{tr}, \end{cases} \quad (62)$$

$$f_{ic-3} = \begin{cases} 0.80 R_{16}^{-\frac{2}{7}}, & R < R_{tr}, \\ 0.44 R_{16}^{\frac{5}{8}}, & R > R_{tr}. \end{cases} \quad (63)$$

As discussed above, we include only the inter-eddy medium for calculating the synchrotron component of the emission, but we include both the eddies and the inter-eddy medium when calculating the IC component. The synchrotron cooling time given by equation (61) applies only to electrons in the inter-eddy medium; the timescale is larger by a factor of  $\gamma_t$  for electrons in eddies. We note that the IC flux should be increased by a factor of 2.5 to allow for the expansion of the source shell (Appendix A). Also, the flux will be larger by a factor  $N_{ed}\gamma_t^3/N_i$  than given in equation (63) if there are more electrons in eddies than in the inter-eddy medium.

### 5.1. Relativistic turbulence: a consistent model for GRB 080319B

Figure 2 is similar to Fig. 1, but shows what happens when we use the relativistic turbulent model. We find a very good match both with the observations and with various consistency conditions when we choose  $R \approx 10^{17}$  cm. For this choice of  $R$ , we have (i)

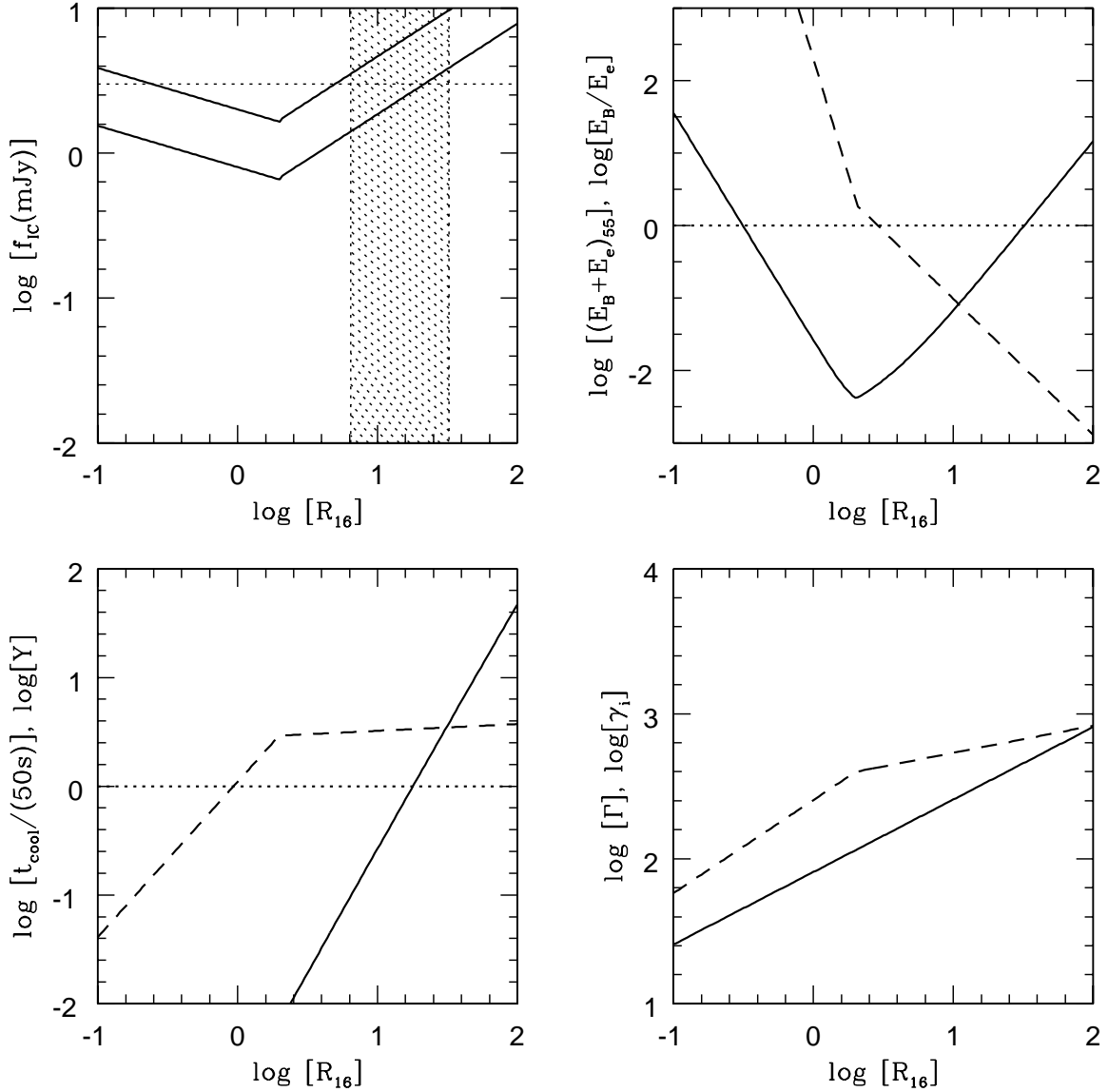


Fig. 2.— Similar to Fig. 1, but for the relativistic turbulence model. Note that the predicted IC flux (solid lines in the top left panel) is perfectly consistent with observations (horizontal dotted line). The shaded region indicates the range of source radii  $R_{16}$  that is consistent with constraints on the total energy (solid line in the top right panel) and the cooling time (solid line in the bottom left panel) constraints (see text for details). We note that the ratio of IC and synchrotron luminosities is larger by  $\sim 10$  than the value of  $Y$  shown as a dashed line in the lower left panel (see eq. 9 for the definition of  $Y$ ) due to two different effects each contributing a factor  $\sim 3$ ; (1) the commonly used Compton- $Y$  is larger than  $Y$  in eq. 9 by a factor 3 due to  $p$  dependent factors, and (2) the synchrotron photon energy density inside the shell is larger than the naive estimate of  $L_{\text{syn}}/(4\pi R^2 c)$  by a factor  $\sim 3$ .

gamma-ray flux  $f_{ic-3}$  predicted to be close to the observed flux, (ii) modest requirement for the total isotropic energy  $\sim 10^{54}$  erg, (iii)  $E_B \sim E_e/10$ , i.e., approximate equipartition between magnetic and thermal energy, (iv)  $t_{cool} \sim 50$  s, i.e., the cooling time is comparable to the burst duration and thus consistent with efficient radiation, (v)  $Y \sim \text{few}^9$ , i.e., consistent with gamma-rays dominating the emission, (vi)  $\Gamma \sim 250$  as inferred for GRBs in general from a variety of observations (Lithwick & Sari, 2001), and (vii) electron Lorentz factor in the inter-eddy medium  $\gamma_i \sim 500$  and in eddies  $\gamma_i/\gamma_t \sim 50$ , which are quite reasonable.

The shaded band in Fig. 2 shows the range of  $R_{16}$  that is consistent with our two primary constraints. First, we require the total isotropic energy over the duration of the burst to be no larger than  $10^{55}$  erg. This constrains  $R_{16}$  to lie in the range  $0.31 - 32$ . Second, we require the cooling time  $t_{cool}$  to lie within a factor of 10 of the burst duration 50 s. This gives the constraint  $6.5 < R_{16} < 50$ . Requiring both conditions to be satisfied simultaneously restricts  $R_{16}$  to lie in the range  $6.5 - 32$ , as shown in Fig. 2. Within this range, the predicted gamma-ray flux agrees remarkably well with observations.

Note that the deceleration radius for the blast wave is

$$R_d = \left( \frac{3E\delta t}{4\pi\bar{n}m_p c(1+z)} \right)^{1/4} = 1.1 \times 10^{17} \text{cm} E_{54}^{1/4} (\delta t/50\text{s})^{1/4} \bar{n}^{-1/4}, \quad (64)$$

where  $\bar{n}$  is the mean particle density of the circumstellar medium within the radius  $R_d$ . It is interesting that  $R_d$  lies in the middle of the allowed range for the source distance  $R$ . It provides independent confirmation that the prompt radiation in GRB 080319B was not produced in internal shocks – there is no reason why internal shocks should occur at the deceleration radius.

In addition to the various successes described above, the relativistic turbulence model explains all the major qualitative features observed in the  $\gamma$ -ray and optical lightcurves of GRB 080319B during the initial  $\sim 10^2$  s, i.e., before the onset of forward shock emission.

Since the gamma-ray emission (via IC) arises partly from eddy electrons and partly from the inter-eddy medium, we expect the gamma-ray lightcurve to consist of a smooth slowly-varying component plus a large number of sharp spikes. This is the case for most GRBs, including GRB 080319B (e.g., Fig. 1 in Racusin et al. 2008). The relative fluxes in the two components provide information on the relative numbers of electrons in the two

---

<sup>9</sup>The ratio of energies in the IC radiation and the synchrotron emission is  $\sim 10Y$ . This is in part because the parameter  $Y$ , defined in eq. 9, differs from the commonly used Compton- $Y$  parameter by a factor  $\sim 3$  (due to  $p$ -dependent factors not included in eq. 9), and the mean synchrotron photon energy density in the shell is larger than  $L_{syn}/(4\pi R^2 c)$  by a factor 3.

media. We assumed in our model (for convenience) that the numbers are roughly equal and this is reasonably consistent with the observations. As already mentioned, by combining the  $\gamma$ -ray variability time of  $\sim 0.5$ s with the burst duration of 50s, we infer that  $\gamma_t \sim 10$  for GRB 080319B.

Since the synchrotron emission is generated by inter-eddy electrons, the optical light curve is expected to be much less variable than the IC-dominated gamma-ray emission. This is indeed the case for GRB 080319B. At the same time, the overall duration of the optical and gamma-ray lightcurves are expected to be similar, as observed.

The optical lightcurve of GRB 080319B showed an initial rapid rise by more than an order of magnitude in flux (Fig. 3 in Racusin et al. 2008), whereas the  $\gamma$ -ray lightcurve showed a much less rapid rise. This finds a natural explanation. According to the turbulent model of GRB 080319B, the synchrotron frequency  $\nu_i$  was below the optical band. Therefore, the optical spectrum is predicted to be very soft:  $F_\nu \propto \nu^{-2.8}$ . If we assume that  $\nu_i$  initially started off at a somewhat lower frequency and later settled down at a larger value, say by a factor of  $\sim 3$ , then the optical flux would increase by nearly a factor of 20. This explanation might indicate that the gamma-ray peak energy  $\nu_{ic}$  should also increase with time, whereas in fact  $\nu_{ic}$  decreased by a small amount (from 750 keV to 550 keV). To explain this, we would need to invoke that the electron Lorentz factor  $\gamma_i$  decreased by a factor of about 2 during this time. Note that the reason for the much less rapid increase of the  $\gamma$ -ray flux is that the synchrotron peak flux, which is proportional to the number of electrons and the magnetic field strength, is a slowly varying function of time.

Another property of the relativistic turbulence model is that we should continue to see emission in the  $\gamma$ -ray band for a time duration somewhat longer than the prompt optical lightcurve duration. The reason is that there is a very high probability that a few eddies lying a little bit outside of  $\Gamma^{-1}$  will point toward the observer, thereby slightly lengthening the burst duration in the gamma-ray band (see Fig. 1 in Narayan & Kumar, 2008). This effect is clearly seen in the lightcurves of GRB 080319B; the optical LC started falling off at 43s whereas the steep decline of the gamma-ray LC began at 51s.

A prediction of the model is that the synchrotron and IC spectra should be the same. In particular, since our solution for GRB 080319B requires  $R \sim 10^{17}$  cm  $> R_{tr}$ , or  $\nu_i < 2$  eV, the spectral index in the optical band during the burst should have been the same as the high energy index in the gamma-ray band, i.e.  $\beta = 2.87$ . It is unfortunate that there were no measurements of optical spectrum during the burst. The first measurement was at  $t \sim 10^2$  s when it was found that  $\beta = 0.55$  or  $f_\nu \propto \nu^{-0.55}$  (Wozniak et al. 2008). This measurement would seem to call into question the prediction of the SSC model.

It is, however, interesting to note that the optical lightcurve showed a sharp break at about 90s. Prior to this time the flux scaled as  $t^{-5.5}$  and after this time the flux decreased as  $t^{-2.8}$  (see Fig. 2 of Kumar & Panaitescu or Racusin et al. 2008). This suggests that 90s marked a transition from one source of radiation to another, and that  $\beta = 0.55$  at  $\sim 10^2$ s corresponds to the second source which gave rise to the  $f_\nu \propto t^{-2.8}$  part of the lightcurve and possibly unrelated to the prompt radiation.

The optical lightcurve decline of  $t^{-5.5}$  between 43s and 90s is roughly consistent with the expectation of the relativistic turbulence model after the source is turned off at  $t \sim 43$ s; the observed radiation in this case is the large-angle emission (LAE) from photons arriving from angles larger than  $\Gamma^{-1}$ , leading to a flux decline of  $t^{-2-\beta}$  or  $\sim t^{-5}$  when  $\beta \sim 3$  (Kumar & Panaitescu, 2000). So the steeply declining optical lightcurve at the end of the GRB provides an indirect confirmation of a steep spectrum in the optical band. We note that the temporal behavior of flux from an adiabatically expanding shell of angular size  $\Gamma^{-1}$  is similar to the large angle emission. The decay index of the lightcurve for adiabatic expansion is somewhat steeper than LAE for a given  $\beta$  (Barniol-Duran & Kumar, 2008), and therefore this is a preferred mechanism for the observed optical flux during 43–90s.

The gamma-ray lightcurve in the 15-150 keV at the end of the burst was seen to fall off even faster than the optical flux at the end of the burst. This is a puzzling behavior, and unlikely to be due to LAE. The reason is that the spectral index in this band was close to zero during the burst, and therefore the LAE flux decline should be  $\sim t^{-2}$  — unless the peak frequency fell off from 650 keV to less than 100 keV at the end of the burst which seems unlikely. The only natural explanation for the steep decline of the  $\gamma$ -ray flux is that the angular size of the source was  $\sim \Gamma^{-1}$ , and gamma-rays for  $t > 51$ s were from the adiabatically cooling source; the IC flux from an adiabatically cooling shell declines much faster than the synchrotron lightcurve (Barniol-Duran & Kumar, 2008).

What about the fall-off of the optical flux as  $t^{-2.8}$  for  $t \gtrsim 10^2$  s? It cannot be LAE for the reasons described above. We offer an explanation for this part of the optical lightcurve that requires the GRB jet to be a Poynting outflow (see §5.2.4). A Poynting jet traveling outward from the center of the star cannot avoid sweeping up and accumulating some amount of baryonic material at its head. In subsequent jet expansion this baryonic gas is cooled, and at the deceleration radius it is heated once again by the reverse shock. The optical emission from this reverse-shock heated gas might be responsible for the lightcurve for  $10^2 \lesssim t \lesssim 10^3$  s. We know from equation (68) below that  $N_e/N_{RS} \sim 10$  (assuming that the kinetic energy in the baryonic head of the Poynting jet is of order the explosion energy). Therefore, the optical flux from the reverse shock is a factor  $\sim 10$  smaller than the prompt gamma-ray source. The more slowly declining reverse shock flux took over from the very rapidly declining flux from



the early GRB tail at  $t \sim 10^2$  s, and continued to dominate the lightcurve until the even more slowly declining, but weaker, forward shock optical emission took over at  $t \sim 10^3$  s. We note that the effect of a narrow jet, with opening angle  $\sim \Gamma^{-1}$ , is very weak on the emergent lightcurve decay for a long period of time when the jet is propagating in a medium with density falling off as  $r^{-2}$  (Kumar & Panaitescu, 2000); the density in the circumstellar medium of GRB 080319B is in fact inferred to be  $r^{-2}$  by the late time afterglow data, cf. Racusin et al. (2008), Kumar & Panaitescu (2008).

## 5.2. Where exactly is the turbulent region located?

As we have seen, the relativistic turbulence model gives robust estimates for various source parameters such as the radius, bulk Lorentz factor and energy of the shell, the number and typical Lorentz factors of the radiating electrons, etc. Using these results we now attempt to infer where the radiating region is located within the context of a dynamical model of GRBs.

### 5.2.1. Not in internal shocks

The internal shock model, including all reasonable variations, is firmly ruled out, as we have discussed in §4. Inclusion of relativistic turbulence within the context of this model will not salvage the situation unless we take  $\delta t$  to be the burst duration (as shown in §5). However, in that case we are dealing with a situation in which the emission region is close to the deceleration radius, which is no longer an internal shock.

The primary motivation for the internal shock model is to explain the rapid variability observed in the gamma-ray lightcurves of GRBs (Sari & Piran 1997). The relativistic turbulence model described in Narayan & Kumar (2008) has a completely different explanation for the variability. In particular, this model no longer needs to assume equation (4), which is the key relation in the internal shock model. Therefore, we see no reason to retain the internal shock picture.

### 5.2.2. Not in the forward shock

In the standard model of GRBs, the collision of the relativistic ejecta with the external medium causes a pair of shocks to be generated: a *forward shock* (FS) which is driven into the external medium and a *reverse shock* (RS) which is driven into the ejecta.

We can rule out the FS by considering the number of electrons we need for producing the observed radiation. From equation (57) we see that the radiating region must have about  $6 \times 10^{54}$  electrons. However, the number  $N_{FS}$  of electrons/protons processed in the FS must satisfy, by a simple energy argument,

$$N_{FS}\Gamma^2 m_p c^2 = E/2, \quad \text{or} \quad N_{FS} = \frac{2E(\delta t)}{m_p c(1+z)R} = 2 \times 10^{52} E_{54}(\delta t)_1(1+z)^{-1} R_{16}^{-1}. \quad (65)$$

For the particular case of GRB 080319B this gives  $N_{FS} \sim 10^{52}$ , which is smaller than the number of electrons needed by a factor  $\sim 10^2$ . This is a large discrepancy, so we can discard the FS as the location of the relativistic turbulence.

### 5.2.3. Relativistic turbulence in the reverse shock?

Could the relativistic turbulence be located in the RS? Let the GRB ejecta be composed of protons and electrons, and let us take the Lorentz factor of the RS front with respect to the unshocked ejecta to be  $\Gamma_{RS}$ . By applying pressure equilibrium across the contact discontinuity between the FS and RS fluid, we find the number of electrons  $N_{RS}$  that have been processed through the RS to be

$$N_{RS} = N_{FS} \frac{\Gamma}{\Gamma_{RS}}. \quad (66)$$

Using equations (55) & (65), and the parameters for GRB 080319B, we find

$$N_{RS} = 1.3 \times 10^{54} E_{55} R_{17}^{1/2} \Gamma_{RS,1}^{-1}. \quad (67)$$

Thus, the ratio of the number of electrons needed for optical/gamma-ray radiation (eq. 57) and  $N_{RS}$  is given by

$$\frac{N_e}{N_{RS}} = 5 E_{55}^{-1} \Gamma_{RS,1}^{-1} R_{17}^{19/16}. \quad (68)$$

If gamma-rays were to arise in the reverse shock then we expect  $E_{55} \sim 0.4$ . The reason is that half the energy of the blast wave is in the reverse shock at the deceleration radius, and this energy is efficiently radiated when the cooling frequency is close to  $\nu_i$ , as seems to be the case for GRB 080319B. Moreover, we presumably require  $\Gamma_{RS} \gtrsim 10$  in order for the shocked gas to have a turbulent  $\gamma_t \sim 10$ . The requirement that  $t_{cool} \sim 50$  s means that  $R_{17} \sim 1$ . Therefore, we find from the above equation that  $N_e/N_{RS} \sim 10$ . This ratio might be closer to unity provided that protons carry a much larger fraction of the blast wave energy, so that  $E_{55}$  is  $\sim 1 - 2$  rather than 0.4.

The interesting result that it is possible to have  $N_e \sim N_{RS}$  suggests that the turbulence is perhaps produced in the RS-heated GRB ejecta. The ratio of energies in magnetic fields and particle kinetic energy in this case is  $\sim 0.1$  (fig. 2), which is similar to the value derived for the Crab pulsar at the wind termination shock (Kennel & Coroniti, 1984). Presumably, the turbulence is a natural consequence of a relativistic shock. For instance, the contact discontinuity surface separating the FS and RS region is known to suffer from the Rayleigh-Taylor instability. Could this explain the turbulence? In the shell comoving frame, the growth rate of the Rayleigh-Taylor instability at the interface of a relativistic RS and FS can be shown to be

$$\omega^2 = fkg, \quad (69)$$

where  $g \sim c^2\Gamma/R$  is the effective gravitational acceleration in the shell comoving frame,  $k = 2\pi\ell\Gamma/R$  is the wavenumber of the perturbation,  $f = 3/(8\Gamma_{RS}^2 - 5)$ , and  $\Gamma_{RS}$  is the Lorentz factor of the RS front with respect to the unshocked ejecta. For  $\Gamma_{RS} \gg 1$  the above equation reduces to

$$\omega \sim \frac{c\Gamma\ell^{1/2}}{\Gamma_{RS}R} \sim \frac{\ell^{1/2}}{\Gamma_{RS}\delta t'}, \quad (70)$$

where  $\delta t'$  is the GRB duration in the shell comoving frame. Thus, the number of e-folds by which the Rayleigh-Taylor mode can grow is  $\sim \omega(\delta t') \sim \ell^{1/2}\Gamma_{RS}^{-1}$ . The eddy scale  $\ell$  of interest to the IC problem is  $R/(\Gamma\Gamma_{RS})$  or  $\ell \sim \Gamma_{RS}$ . Perturbations on this scale will undergo  $\Gamma_{RS}^{-1/2}$  e-folds of growth, i.e., the amplitude increases by less than a factor 2. Therefore, the Rayleigh-Taylor instability is not sufficiently potent to generate the highly relativistic turbulence we need.

Recently Goodman & MacFadyen (2007) and Milosavljevic, Nakar & Zhang (2007) have discovered interesting instabilities, resulting from a clumpy circumstellar medium and an initially anisotropic blastwave respectively, which lead to vorticity generation downstream of the shock front. These instabilities have been further studied by Sironi & Goodman (2007), and Milosavljevic et al. (2007) to investigate the generation of magnetic fields in relativistic shocks. Couch, Milosavljevic & Nakar (2008) have found another instability that generates vorticity down stream of a shockfront even when the circumstellar medium is homogeneous and the blastwave isotropic. We have estimated the growth rate of these instabilities and find that these too fail to give rise to relativistic turbulence.

Of course, we cannot rule out the possibility that there might be other as yet unknown instabilities that might give rise to relativistic turbulence. Therefore, we are unable to discard the possibility that the prompt GRB emission originates in the RS.

#### 5.2.4. *Relativistic turbulence in the Poynting-dominated jet*

A Poynting-dominated jet would have a weak reverse shock (Kennel & Coroniti, 1984; Zhang & Kobayashi, 2005) and would not be consistent with the proposal considered in the previous subsection. On the other hand, such a jet probably undergoes various plasma instabilities at the deceleration radius. These instabilities would stir up the fluid into a state consistent with our model of relativistic turbulence. The instabilities would presumably heat up the electrons until quasi-equipartition is achieved, consistent with the results shown in Fig. 2.

According to equations (59) & (60), in our model  $E_B/E_e \sim 0.1$  at  $R \sim 10^{17}$  cm. However, this does not rule out the Poynting outflow model. The reason is that in all of our formulae  $B$  really stands for the projection of the magnetic field vector perpendicular to the electron momentum vector i.e.,  $B \sin \alpha$  where  $\alpha$  is the pitch angle between the electron momentum and the magnetic field direction. For a random distribution of particle pitch angle the difference between  $B$  and  $B \sin \alpha$  is order unity. However, when electrons have a non-zero average momentum along the local magnetic field (as might be the case for particles accelerated in reconnection regions), the difference can be large. For instance, when the average  $\alpha$  is 0.3 the energy in magnetic fields is larger than that in equation (59) by a factor  $\sim 10$ , making the model consistent with equipartition.

Lyutikov and Blandford (2003) have suggested that the dissipation of magnetic energy in a Poynting flux dominated jet should occur at a distance of  $\sim 3 \times 10^{16}$  cm due to current driven instabilities (see Lyutikov 2006 for a concise summary of the model, and for a comparison with the baryonic outflow model). Acceleration of electrons (and positrons), and plasma bulk flow along the magnetic field lines at roughly the local Alfvén speed are expected in the process of magnetic field decay/reconnection. These expectations of the Poynting outflow model are roughly consistent with our findings for GRB 080319B: emission generated at  $R \approx 10^{17}$  cm and turbulent velocity field with Lorentz factor  $\gamma_t \sim 10$ . However, the reason for a very soft particle spectrum,  $p \sim 5$ , is unclear (at least to us); numerical simulations of particle acceleration in reconnection regions generally find a hard particle spectrum (e.g., Larrabee et al. 2003).

Moreover, it is also not clear how  $\gamma_t$  and  $\gamma_i$  should be related to the bulk  $\Gamma$  of the pre-instability jet. Nor is it clear why the typical Lorentz factor of electrons should be a modest value  $\gamma_i \approx 500$  with the kind of powerful accelerator one might expect in magnetic reconnections (other than the fact that it is energetically impossible to accelerate a large number of electrons, of order  $10^{55}$ , to an average Lorentz factor much larger than  $\sim 500$ ). Further investigation is required to address these questions.

## 6. Summary

We have shown in this paper that the gamma-ray and optical data for GRB 080319B rule out the popular internal shock model for generation of the prompt radiation. According to this model, the duration ( $\lesssim 1$  s) of spikes in the gamma-ray lightcurve sets an upper bound on the quantity  $R/(2c\Gamma^2)$ , where  $R$  is the radius of the source relative to the center of the explosion and  $\Gamma$  is the bulk Lorentz factor. When we apply this condition, we find that it is impossible to fit the observed optical and gamma-ray flux simultaneously. Specifically, any model that fits the optical flux under predicts the gamma-ray flux by nearly two orders of magnitude (Fig. 1). This is an unacceptably large discrepancy which cannot be eliminated with any reasonable modification of the internal shock model.

An equally powerful qualitative argument against the internal shock model is the fact that we find the radius  $R$  of the source to be constrained quite tightly by the observations. The energy required in magnetic field increases very rapidly as we decrease  $R$ ,  $E_B \propto R^{-22/7}$ , whereas the energy in particles increases rapidly,  $E_e \propto R^{17/7}$ . Also, the cooling time of electrons becomes too short to be compatible with observations if  $R < 3 \times 10^{16}$  cm.<sup>10</sup> All of these factors together constrain the location where the prompt emission in GRB 080319B was produced to lie within a narrow range of radius:  $4 \times 10^{16} \lesssim R \lesssim 8 \times 10^{16}$  cm (see Fig. 1). This is problematic for the internal shock model. According to this model, there is a large number of internal shocks among independent ejecta, with a separate shock producing each of the  $\sim 50$  spikes in the gamma-ray lightcurve of GRB 080319B. Why would all the ejecta collide within such a narrow range of radius? Moreover, why should the radius be so close to the deceleration radius  $R_d \sim 10^{17}$  cm, where the ejecta meet the external medium and begin to slow down? This coincidence is suspicious.

All of these problems are eliminated if we give up the internal shock model and consider instead a model in which the variability in the gamma-ray lightcurve is produced by relativistic turbulence in the source with random eddy Lorentz factors  $\gamma_t \sim 10$ . In this model, the quantity  $R/(2c\Gamma^2)$  is no longer constrained to be less than 1 s, but only needs to be comparable to the burst duration  $\sim 50$  s (Narayan & Kumar 2008). With this modification, we find that we obtain a remarkably consistent model of GRB 080318B (see Fig. 2) in which the prompt optical emission was produced by synchrotron emission and the gamma-rays

---

<sup>10</sup>Collisions at a smaller radius would produce a weak optical flash with flux decreasing roughly as  $R^{11/12}$ . The electrons would undergo very rapid cooling and produce a low energy spectrum in the gamma-ray band of  $f_\nu \propto \nu^{-1/2}$ . Prompt optical observations of GRB 080319B show variations in the optical flux by less than a factor two for much of the 50s duration of the burst except at the beginning and the end. Moreover, the low energy spectral index for the gamma-ray emission was greater than 0 throughout the burst.

were the result of inverse Compton scattering. The predicted gamma-ray flux is perfectly compatible with observations. Also, estimates of various quantities such as the total energy, cooling time, Lorentz factor, etc. are all very reasonable and consistent (§5.1). The radius of the source is calculated to be in the range  $6 \times 10^{16} < R < 3 \times 10^{17}$  cm; if we select a nominal value  $R \sim 10^{17}$  cm, we obtain an excellent fit to all the observations.

In the context of a physical model, the picture that emerges from this model is that the energy of the relativistic jet in GRB 080319B was converted to optical &  $\gamma$ -ray radiation either via a relativistic reverse shock when ejecta (composed of  $p^+$ s and  $e^-$ s) ran into the circumstellar medium or that much of the jet energy was in magnetic field that was dissipated close to the deceleration radius. Theoretically, it is difficult to understand how a reverse shock might produce relativistic turbulence with  $\gamma_t \sim 10$  (§5.2.3). Also, it is easier to understand the optical data for the time period  $10^2 \lesssim t \lesssim 10^3$  s if we assume a Poynting jet (§5.2.4). For these reasons we have a mild preference for the Poynting-dominated jet model.

A potential problem for the Poynting jet model is that the ratio of magnetic to particle kinetic energy is about 0.1 for our best solution (Fig. 2). However, this ratio is similar to that inferred for the pulsar wind termination shock for the Crab pulsar (Kennel & Coroniti, 1984). Moreover, this ratio of 0.1 does not rule out the Poynting model for another reason which is that, in all of our formulae,  $B$  is the projection of the magnetic field perpendicular to the electron momentum vector. Thus, if electron momenta are preferentially parallel to the magnetic field, then the true  $E_B$  would be larger than our estimate (easily by a factor 10 compared to the value given in eq. 59), and we can have  $E_B/E_e \sim 1$ . Note that electrons are accelerated parallel to the magnetic field in reconnection regions and so this possibility is not as arbitrary as it might appear.

In the relativistic turbulence model, fluctuations in the observed gamma-ray lightcurve are produced as a result of random relativistic variations in the velocity field of the source, with turbulent Lorentz factor  $\gamma_t \sim 10$ . The model predicts that there should be  $\sim \gamma_t^2 \sim 100$  spikes in the gamma-ray light curve (Narayan & Kumar 2008), which is consistent with the  $\sim 50$  spikes seen in GRB 080319B. The optical synchrotron flux is dominated by the inter-eddy medium rather than eddies. Therefore, we expect much less variability in the optical flux, as was indeed observed.

The model can explain the sharp rise in the optical flux of GRB 080319B at the beginning of the burst. For this, we must postulate that the synchrotron peak frequency increased from  $\sim 0.5$  eV to  $\sim 1.5$  eV during the first  $\sim 15$  s. Since the synchrotron peak frequency  $\nu_i$  was below the optical band (2 eV), the optical flux was smaller than the peak synchrotron flux by a factor  $(4/\nu_i)^{2.8}$  (the spectral index above the peak is known from gamma-ray observations). A modest increase in  $\nu_i$  by a factor of 3 early in the burst would thus produce a factor of

20 increase in the observed optical flux. The reason that the gamma-ray flux increased by a much smaller factor during the same time is that the peak IC flux is proportional to  $\tau_e N_e B$ , which would change little during this time period.

The end of the gamma-ray prompt emission phase occurred  $\sim 8$  s after the prompt optical in GRB 080319B. This is probably a result of inverse Compton emission from turbulent eddies lying a bit outside of the primary  $1/\Gamma$  cone, but which happened to point toward us because of a fortuitous alignment of their turbulent velocity (the probability for this happening is of order unity). Since much of the synchrotron emission comes from non-turbulent fluid in between eddies, the optical flux would not have a similar effect.

### Acknowledgments

PK is grateful to Rodolfo Barniol Duran for checking all equations in this paper, and Milos Milosavljevic for a number of useful discussions regarding relativistic turbulence.

### REFERENCES

- Barniol Duran, R. & Kumar, P. 2008, arXiv: 0806.1226
- Couch, S.M., Milosavljevic, M. & Nakar, E. 2008, ApJ 688, 462
- Cucchiara A., Fox D., 2008, GCN 7456\*
- Dermer, C.D., Chiang, J., and Botcher, M., 1999, ApJ, 513, 656
- Golenetskii S. et al., 2008, GCN 7482\*
- Goodman, J. & MacFadyen, A.I. 2007, arXiv0706.1818
- Karpov S. et al., 2008, GCN 7558\*
- Katz, J. 1994, ApJ, 422, 248
- Kennel, C.F. & Coroniti, F.V. 1984, ApJ 283, 694
- Kumar, P. & Panaitescu, A. 2000, ApJ 541, L9
- Kumar, P. & Panaitescu, A. 2000, ApJ 541, L51
- Kumar, P. & Panaitescu, A. 2008, MNRAS

- Kumar, P. & McMahon, E. 2008, MNRAS 384, 33
- Larrabee, D.A., Lovelace, R.V.E. & Romanova, M.M. 2003, ApJ 586, 72
- Lithwick, Y. & Sari, R. 2001, ApJ 555, 540L
- Lyutikov, M. 2006, New J. Phys. 8, 110
- Lyutikov, M. & Blandford, R.D. 2003, astro-ph/0312347
- Mészáros, P. 2002, ARA&A, 40, 137
- Milosavljevic, M., Nakar, E. & Zhang, F. 2007, arXiv: 0708.1588
- Narayan, R. and Kumar, P., 2008, submitted to MNRAS
- Racusin, J. L. et al. 2008, Nature 455, 183
- Rybicki, G.B. and Lightman, A.P., 1979, Radiative Processes in Astrophysics, John Wiley & Sons (New York)
- Piran, T. 1999, Phys. Rep., 314, 575
- Piran, T. 2005, Reviews of Modern Physics, 76, 1143
- Piran, T., Shemi, A. & Narayan, R. 1993, MNRAS, 263, 861
- Rees, M.J. & Meszaros, P. 1994, ApJ, 430, L93
- Sironi, L. & Goodman, J. 2007, ApJ 671, 1858
- Thompson, C. 1994, MNRAS, 270, 480
- Thompson, C. 2006, ApJ, 651, 333
- Usov, V. V. 1992, Nature, 357, 472
- Usov, V. V. 1994, MNRAS, 267, 1035
- Vreeswijk P. et al., 2008, GCN 7444\*
- Wheeler, J.C., Yi, I., Hofflich, P., and Wang, L., 2000, ApJ 537, 810
- Wheeler, J.C., Meier, D.L., and Wilson, J.R., 2002, ApJ 568, 807
- Wijers, R. A. M. J., & Galama, T. J. 1999, ApJ, 523, 177



Wozniak, P.R. et al. 2008, arXiv:0810.2481

Zhang, B. 2007, Chinese Journal of Astronomy and Astrophysics, 7, 1

Zhang, B. & Kobayashi, S. 2005, ApJ 628, 315

### A. Possible errors in the calculation of IC flux

We discuss in this appendix possible sources of error in our calculation of the IC flux, i.e. errors associated with eq. (48); according to this equation the theoretically calculated gamma-ray flux is smaller than the observed value by a factor  $\sim 20$ .

A possible source of error might arise from our assumption of a homogeneous source, and we need to estimate its effect on the IC flux. The synchrotron peak flux is a linear function of magnetic field strength and the total number of electrons in the source, and therefore clumping of electrons and  $B$ , to lowest order, have little effect on the emergent flux. The IC flux is, however, affected by clumping of electrons, and we estimate the magnitude of this effect.

Let us consider an extreme form of inhomogeneity where all electrons are concentrated in  $M_c$  clumps of each size  $r_c$ . The number density of electrons in the clumps is  $n_c$ , and the density averaged over the source volume,  $\sim R^3$ , is  $n_0$ ; there are no electrons in between clumps. Let us assume that the synchrotron power from each electron is  $p_\nu$ . In this case the synchrotron luminosity of the source is

$$L_{syn}(\nu) \approx p_\nu(n_c r_c^3)M_c \approx p_\nu n_0 R^3, \quad (\text{A1})$$

and is independent of electron clumping. The IC luminosity depends on synchrotron flux in the vicinity of electrons (in clumps). The synchrotron flux is

$$f_{syn}(\nu) \approx p_\nu(n_c r_c + n_0 R) \approx \frac{L_{syn}(\nu)}{R^2} \left[ 1 + \frac{n_c r_c}{n_0 R} \right]. \quad (\text{A2})$$

The IC luminosity is obtained from the above flux:

$$L_{ic}(\nu_{ic}) \approx \sigma_T f_{syn}(\nu) n_c r_c^3 M_c \approx \sigma_T L_{syn}(\nu) n_0 R \left[ 1 + \frac{n_c r_c}{n_0 R} \right]. \quad (\text{A3})$$

Or

$$L_{ic}(\nu_{ic}) \approx \sigma_T L_{syn}(\nu) n_0 R [1 + f_c^{-2/3} M_c^{-1/3}], \quad (\text{A4})$$

where  $f_c = n_c r_c^3 M_c / (n_0 R^3)$  is the fraction of the shell volume occupied by clumps. We see from the above equation that IC flux can be enhanced by clumping of electrons. For instance, consider an example where  $f_c = 0.1$  and  $M_c = 1$  (all electrons are in a single small clump). The IC flux in this case is a factor 4.5 larger than when electrons are uniformly distributed. This flux enhancement is about an order of magnitude smaller than what is needed to explain the observed flux for GRB 080319B (eq. 48). An even more extreme case of clumping could bridge the gap, however the efficiency for converting jet energy to radiation is very small when  $f_c \ll 1$  as pointed out by Sari and Piran (1997). Furthermore, another serious problem is that a high degree of clumping leads to an increase of  $\nu_a$  (as discussed below), and that makes the SSC spectrum below the peak inconsistent with the observed data for GRB 080319B – unless we place the source at a distance from the center of explosion that is larger than the deceleration radius.

The dependence of  $f_{ic}$  on  $\eta \equiv \nu_i / \nu_a$  is fairly strong and so we need to discuss the uncertainty in  $\eta$ . We have taken  $\eta = 25$  ( $\log \eta = 1.4$ ), which is guided by the Konus-Wind low energy spectrum of  $f_\nu \propto \nu^{0.2}$  in the energy band 20–650 keV. This low energy spectral index suggests that  $\nu_a$  (the self-absorption frequency) should be  $\lesssim 20$  keV, and thus  $\eta \gtrsim 32$ ; therefore,  $\eta = 25$  is a conservative choice for GRB 080319B. However, is it possible that  $\nu_a$  has been overestimated in our calculation by our assumption of a homogeneous source? If  $\nu_a$  were to be smaller by a factor  $\sim 6$  than given by equation (16) then that would lead to a larger IC flux by factor 30 (see eq. 48), and thereby reconcile the observed and the theoretically expected gamma-ray flux. We show that inhomogeneities in the source cannot decrease  $\nu_a$  as long as the optical flux we observed during the burst is produced in the source.

We calculate synchrotron self-absorption frequency ( $\nu_a$ ) when  $B$ ,  $\gamma_i$  &  $n_0$  are allowed to vary, arbitrarily, across the source; the electron distribution is taken to be  $dn/d\gamma = n_0(\gamma/\gamma_i)^{-p}$  for  $\gamma \geq \gamma_i$ . Spatial variations in  $B$ ,  $\gamma_i$  &  $n_0$  are subject to constraints that the optical flux and the IC peak frequency should be equal to the observed values.

Our starting point is equation (6.52) of Rybicki & Lightman (1979) for the synchrotron absorption coefficient,  $\alpha_\nu$ ;  $\int dr' \alpha_\nu$  is the optical depth for absorbing synchrotron photons of frequency  $\nu$ . We can show that for a power-law electron distribution and for  $\nu < \nu_i$  (the case of interest for 080319B)

$$\alpha_{\nu'} \approx \frac{3^{1/2}(p+2)(p-1)q^3 n_0 B \sin \delta}{16\pi^2(p+2/3)m_e \nu'^2 \gamma_i} \left(\frac{\nu'}{\nu'_i}\right)^{1/3}, \quad (\text{A5})$$

where

$$\nu'_i \equiv \frac{3qB \sin \delta \gamma_i^2}{4\pi m_e c}, \quad (\text{A6})$$

$\delta$  is the angle between magnetic field and electron velocity vector, and prime denotes frequency in the source comoving frame. The synchrotron self-absorption frequency is determined from the equation

$$\int dr' \alpha_{\nu'_a} \approx \frac{3^{1/2}(p+2)(p-1)q^3}{16\pi^2(p+2/3)m_e\nu'_a{}^2} \int dr' \frac{n_0 B \sin \delta}{\gamma_i} \left(\frac{\nu'_a}{\nu'_i}\right)^{1/3} = 1. \quad (\text{A7})$$

Or

$$\nu'_a{}^{5/3} \approx \frac{3^{1/2}(p+2)(p-1)q^3}{16\pi^2 m_e (p+2/3)} \int dr' \frac{n_0 B \sin \delta}{\nu'_i{}^{1/3} \gamma_i}. \quad (\text{A8})$$

The  $\nu'_a$  given by the above equation is self-absorption frequency along one line of sight. Since an observer receives photons from an area  $\sim \pi R^2/\Gamma^2$ , we should average  $\nu_a$  over this area. This average frequency is given by

$$\langle \nu'_a{}^{5/3} \rangle \approx \frac{3^{1/2}(p+2)(p-1)q^3}{16\pi^2 m_e (p+2/3)} \frac{\Gamma^2}{\pi R^2} \int d^3 \mathbf{x}' \frac{n_0 B \sin \delta}{\nu'_i{}^{1/3} \gamma_i}. \quad (\text{A9})$$

Since the optical flux ( $f_{op}$ ) is proportional to  $\int d^3 \mathbf{x}' n_0 B \sin \delta / \nu'_i{}^{1/3}$ , when  $\nu'_i$  lies above the optical band, it is convenient to define a new variable  $\chi \equiv n_0 B \sin \delta / \nu'_i{}^{1/3}$ , and rewrite the equation for  $\nu'_a$  using this new variable

$$\langle \nu'_a{}^{5/3} \rangle \propto \frac{1}{R^2} \int d^3 \mathbf{x}' \frac{\chi}{\gamma_i}. \quad (\text{A10})$$

The minimum of  $\nu'_a$  can be obtained by requiring that  $\delta \nu'_a = 0$  for an infinitesimal variation of  $\chi(\mathbf{x}')$ , i.e.

$$\int d^3 \mathbf{x}' \frac{\delta \chi(\mathbf{x}')}{\gamma_i(\mathbf{x}')} = 0, \quad (\text{A11})$$

subject to the condition that

$$\int d^3 \mathbf{x}' \delta \chi(\mathbf{x}') = 0. \quad (\text{A12})$$

The variational integral implicitly assumes that we are solving for  $\gamma_i(\mathbf{x}')$  which can be an arbitrary function as long as the IC spectral peak of the radiation emergent from the source matches the observed value, i.e.  $1 \ll \gamma_i \ll \infty$ . Let us consider a special form of  $\delta \chi(\mathbf{x}')$  that is nonzero in two spherical regions of infinitesimal radius centered at  $\mathbf{x}'_1$  and  $\mathbf{x}'_2$ . It is required that  $\delta \chi(\mathbf{x}'_1) = -\delta \chi(\mathbf{x}'_2)$  in order to satisfy the optical flux constraint. Substituting this into equation (A11) leads to  $\gamma_i(\mathbf{x}'_1) = \gamma_i(\mathbf{x}'_2)$ . Since,  $\mathbf{x}'_1$  and  $\mathbf{x}'_2$  were arbitrary points

in the source, we conclude that  $\gamma_i$  does not vary across the source when  $\nu'_a$  is minimized. Therefore, we can take  $\gamma_i$  outside of the integral in equation (A10), and find see that the minimum value of  $\langle \nu_a \rangle$  is fixed by the observed optical flux. In other words, the assumption of a homogeneous source used in our calculations in §3 & §4 gives the smallest possible value for  $\eta$  or the largest IC flux. For a high degree of clumping of electrons in the source, we considered above,  $\nu_a$  is larger when our line of sight passes through a clump and especially when only one clump lies on our sight line; there is, however, little change to  $\langle \nu_a \rangle$  as we have shown above. In this case an observer will receive radiation from one clump at a time, and will find  $\nu_a$  larger than the case of a homogeneous shell. A larger  $\nu_a$  for a clumpy source goes in the opposite direction to what we need to increase the IC flux, and this largely reverses the gain to the IC flux found above (eq. A4).

We assumed in our derivation that  $\nu'_i$  is above the optical band. A similar proof for the minimum of  $\nu'_a$  can be carried out when  $\nu'_i$  is below the optical frequency. Moreover, we ignored variations of  $\Gamma$  across the source. This approximation is justified since large variation in  $\Gamma$  are smoothed out in less than one dynamical time.

There is one effect that we have not included in our calculation which lowers the value of the self-absorption frequency  $\nu_a$  somewhat. As synchrotron photons propagate outward they move through a medium where the electron density is decreasing with time (due to the outward expansion of the shell). As a result, a calculation based on a stationary source overestimates the optical depth to Thomson scattering and  $\nu_a$  by factors of  $\sim 2$  &  $\sim 2^{3/5}$ , respectively. This can be seen by considering a homogeneous shell with electron density  $n_0$  located at a distance  $R_0$  from the center of explosion, with a radial thickness  $R_0/\Gamma^2$ . (The comoving frame shell thickness of  $R_0/\Gamma$  is obtained by causality considerations, since  $R_0/c\Gamma$  is the time elapsed in the shell comoving frame.) As seen by a lab frame observer, a photon moving outward in the radial direction takes a time  $2R_0/c$  to cross the shell, and during this time the shell has moved to a larger radius and the density has decreased. For a hot shell, the radial width too increases with time, and the photon transit time is a bit larger still. A straightforward calculation of the optical depth to Thomson scattering when the density changes as  $1/R^2$  shows that the shell optical depth is about half of what it is for a stationary medium of the same thickness and density. Substituting this optical depth into equation (A8) for  $\nu_a$  we see that the synchrotron-self absorption frequency is smaller for an expanding shell by a factor of  $\sim 2^{3/5}$ .

The net effect is that the parameter  $\eta$  which is defined in equation (17) should be reduced by a factor of  $2^{3/5}$ . In the case of GRB 080319B, we estimated  $\eta \sim 25$  from the observations. We should use a smaller value  $\eta \sim 16$  in our formulae to obtain more accurate numerical estimates of quantities. This causes the predicted gamma-ray flux to be increased

by a factor of 2.5.